Global Validation of Altimetric Variables, Corrections, and Editing

Remko Scharroo and John Lillibridge

Final Report to the ENVISAT RA-2/MWR Cross-Calibration/Validation Team
May 2003

NOAA Laboratory for Satellite Altimetry
1335 East-West Highway: E/RA31
Silver Spring, MD 20910

Table of Contents

Abstract

Global distribution plots and two-dimensional histograms are utilized to perform global validation of the Envisat GDR product suite. Environmental corrections and the primary altimetric variables are assessed. Editing criteria based on these corrections and variables are evaluated along with flag bit edits. Recommendations for improvement of the Envisat data, algorithms, and processing procedures are presented.

1. Analysis Datasets

The cross-calibration of Envisat and ERS-2 altimeter and radiometer data was performed using three 35-day cycles of coincident observations. ERS-2 cycles 78 - 80 were compared with Envisat cycles 10 - 12. The time span of the data covers 2002/09/30 22:08:08 – 2003/01/13 21:57:47 for ERS-2 and 2002/10/04 00:23:36 – 2003/01/13 21:34:17 for Envisat.

The ERS-2 data were comprised of OPR02 records from the F-PAC. We tried to follow the guidelines for a 'standard recipe' for treatment of the OPR data based on "OPR and WAP standard products for cross-calibration with Envisat RA-2/MWR", J. Benveniste and A. Martini, PO-TN-ESR-RA-0056, 23 January 2001. To summarize, the specific changes we implemented:

1. USO timing and SPTR range corrections from the ESRIN database (A. Martini and P. Femenias, "The ERS SPTR2000 Altimetric Range Correction: Results and Validation", ESA ERE-TN-ADQ-GSO-6001, Nov 2000).
2. 23.8 GHz brightness temperatures corrected for gain loss and drift (L. Eymard and S. A. Boukabara, "MWR2 anomaly. Proposal for correction". CETP report, 13 November 1996. ; L. Eymard, E. Obligis, and N. Tran, "ERS-2/MWR long-term survey", Ref. CLS/DOS/NT/03.688, CLS, Ramonville, France, February 2003).
3. 1.5 millisecond timing bias applied to range (R. Scharroo, "A Decade of ERS Orbits and Altimetry", Delft, The Netherlands, December 2003).
4. Backscatter (sigma-0) corrected for variations since Jan. 2000 (J. Dorandeu, F. Mertz, J. Stum, "Note of ERS-2 Sigma0 variations since January 2000", CLS/DOS/NT/00.286, CLS, Ramonville, France, August 2000).

The Envisat data were generated by the FRAPPE processor at ESRIN as a special service to the CCVT effort. The data set is essentially a final F-PAC/SSALTO/CMA Level-2 GDR product in terms of format and content (reference: PO-RS-MDA-GS-2009_V/I3L). No changes were made initially to the Envisat data except where noted below.

An essential part of the cross-calibration exercise is to insure consistency of the environmental corrections to the range measurement for the two missions, and to utilize model wet troposphere and ionosphere corrections (rather than measured instrument values) since the radiometer and dual-frequency ionosphere are to be calibrated separately. We closely followed the procedures in the 'standard recipe' but in some cases upgraded to the latest model corrections (for Envisat and the other altimeters considered) as shown in Table 1. This Table also lists some of the alternative corrections that were used to correct the Envisat data.

Table 1. Environmental corrections to altimeter range.

Mission	Orbit	Dry troposphere	Wet troposphere	Ionosphere	Inverse barometer	Solid tide	Ocean & load tide	Pole tide	SSB	MSS
ERS-2	DEOS GRIM-5C1	ECMWF	ECMWF (Cartesian)	JPL-GIM	ECMWF – Global ocean mean	Cartwright & Edden	GOT00.2	DEOS	Gaspar & Ogor	CLS MSS01
TOPEX	NASA	ECMWF	ECMWF	JPL-GIM	ECMWF – Global ocean mean	Cartwright & Edden	GOT00.2	DEOS	BM4	CLS MSS01
Jason-1	CNES	ECMWF	ECMWF	JPL-GIM	ECMWF – Global ocean mean	Cartwright & Edden	GOT00.2	DEOS	BM3	CLS MSS01
GFO	NASA	ECMWF	ECMWF	JPL-GIM	ECMWF – Global ocean mean	Cartwright & Edden	GOT00.2	DEOS	BM3	CLS MSS01
Envisat	DEOS GRIM-5C1	ECMWF	0.958 * ECMWF (Gaussian)	JPL-GIM	ECMWF – Global ocean mean	Cartwright & Edden	GOT00.2	DEOS	BM3	CLS MSS01
Others tested for Envisat	CNES		ECMWF wet, MWR wet	DORIS; Dual-frequency					NOAA hybrid model	

The raw ERS-2 OPR and Envisat GDR datasets were read into the Delft RADS database (http://www.deos.tudelft.nl/altim/rads/rads.shtml) that we've implemented at NOAA/LSA. A prime benefit of using RADS is the certainty that the environmental corrections applied to the two missions' datasets are internally consistent and state-of-the-art models are used. As shown in Table 1, we have followed the guidelines of the 'standard recipe' for consistency, but have utilized newer models than those initially recommended: GRIM-5C1 orbits computed by DEOS, JPL-GIM (vs. Bent) model ionosphere; GOT00.2 ocean and load tide model; and the CLS MSS01 mean sea surface. We have also chosen to apply the small pole tide correction, a byproduct of the orbit determination at DEOS.

2. Editing

Edit criteria for the computation of fully-corrected sea surface height anomaly (orbit - range - environmental corrections - mean sea surface) also need to be applied consistently for both ERS-2 and Envisat. There are three sources of edit criteria: limits on the environmental corrections used to correct the range; limits on altimetric parameters independent of range; and flag bits generated by the data processing chains.

In the RADS processing we can easily specify the limits on the corrections and other variables associated with the corrected SSH anomaly values. If any variable exceeds the minimum or maximum limits, or any editing flag bit is set, the SSH anomaly is discarded from further analysis.

Table 2 and Table 3 present the limits used in our cross-calibration study. In most instances the same values apply to both ERS-2 and Envisat. Where they differ the values in the table cells are separated by a '/'. Most notably, due to an overall bias in the Envisat data, the limits on the final SSH anomaly are offset by a meter for Envisat vs. ERS-2. The upper limit on the wet troposphere correction was set to a positive value to accommodate a bias in the MWR wet troposphere (discussed further below).

Table 2 presents the edit limits, and percentage of data edited for each 35-day cycle, based on the environmental corrections to range: wet and dry troposphere, ionosphere, inverse barometer, tides, and sea state bias. The min. and max. limits in the first two rows are generally RADS defaults aside from the exceptions noted above. Each of the edit criteria are evaluated independently, *i.e.*, many

editing points are commonly edited by several different corrections. This explains the most obvious feature of the table: the large percentage of edited Envisat data compared to ERS-2. The Envisat data are 'all surface' so we have a large amount of land and ice data prior to editing. By contrast the ERS-2 OPR data are ocean-only. For example the non-zero values for dry troposphere and inverse barometer edits for Envisat arise when the land elevation reduces the surface pressure values, resulting in small negative values for these corrections which are outside the edit limits. Similarly ocean tides are undefined over land in the Envisat GDRs. Generally the environmental correction editing amounts to just a few percent of the over-ocean data.

Table 3 includes editing based on altimetric parameters as well as flag bits. Again the land values make Envisat appear to have many more bad points, but it is apparent that these edit criteria are the ones that are removing most of the bad over-ocean data points. In the past, as we do here for ERS-2, the combination of incomplete frames (number of points < 17), limits on sigma-SSH and sigma-SWH, and flag bits was an effective edit combination. For Envisat, however, the robust and agile on-board tracker returns reasonably small values for sigma-SSH and sigma-SWH even over sea-ice and rain-contaminated regions.

Fortunately the peakiness parameter in the FD/I/GDRs (but not currently in the FD/IMARs) can be used as an additional editor for sea-ice and to a lesser extent rain. Figure 1 shows the distribution of peakiness for cycles 10-12 of Envisat, with values outside the edit range of 1.5-1.8 shown in red. Clearly over-land and sea-ice values are discriminated by peakiness. It is estimated that roughly 5% of sea-ice values might fall within the 1.5-1.8 range with some seasonal variation [S. Laxon, pers. comm.].

Table 2. Edit limits on environmental corrections.

Correction:	Dry tropo	Wet troposphere	Ionosphere	Inverse barometer	Solid tide	Ocean tide	Load tide	Pole tide	SSB
Maximum	-2.1 m	+0.05/0.0 m	+0.04 m	+1.0 m	+1.0 m	+5.0 m	+0.5 m	+0.1 m	+1.0 m
Minimum	-2.4 m	-0.6 m	-0.4 m	-1.0 m	-1.0 m	-5.0 m	-0.5 m	-0.1 m	-1.0 m
%edit: c10/c78	12.9/0.0	0.0/0.2	0.0/0.0	11.9/0.0	0.0/0.0	31.4/1.2	0.0/0.0	0.0/0.0	0.3/0.1
%edit: c11/c79	12.9/0.0	0.0/0.3	0.0/0.0	11.9/0.0	0.0/0.0	31.4/1.4	0.0/0.0	0.0/0.0	0.3/0.1
%edit: c12/c80	13.1/0.0	0.0/0.3	0.0/0.0	12.0/0.0	0.0/0.0	31.5/1.4	0.0/0.0	0.0/0.0	0.2/0.1

Table 3. Edit limits on altimetric parameters.

Parameter:	SSH anomaly	1-Hz σ_{SSH}	SWH	1-Hz σ_{SWH}	σ_0	Wind	Peakiness	# 18 Hz points	Flags
Maximum	+6.0/+5.0 m	+0.09 m	+8.0 m	+0.5 m	+27 dB	+30 m/s	+1.8/-	20	See below
Minimum	-4.0/-5.0 m	0.0 m	0.0 m	0.0 m	+6 dB	0 m/s	+1.5/-	17	See below
% edit: c10/c78	69.1/11.8	32.7/7.3	17.4/1.0	28.0/7.1	16.1/0.2	0.3/0.0	39.9/-	5.3/7.9	64.1/4.4
% edit: c11/c79	49.5/14.4	32.4/7.7	18.0/1.3	28.0/7.3	16.5/0.2	0.3/0.1	39.8/-	4.9/8.5	42.7/6.7
% edit: c12/c80	51.2/11.2	31.8/7.2	18.9/1.2	28.0/6.9	17.2/0.3	0.2/0.1	38.9/-	4.8/7.8	44.7/3.8

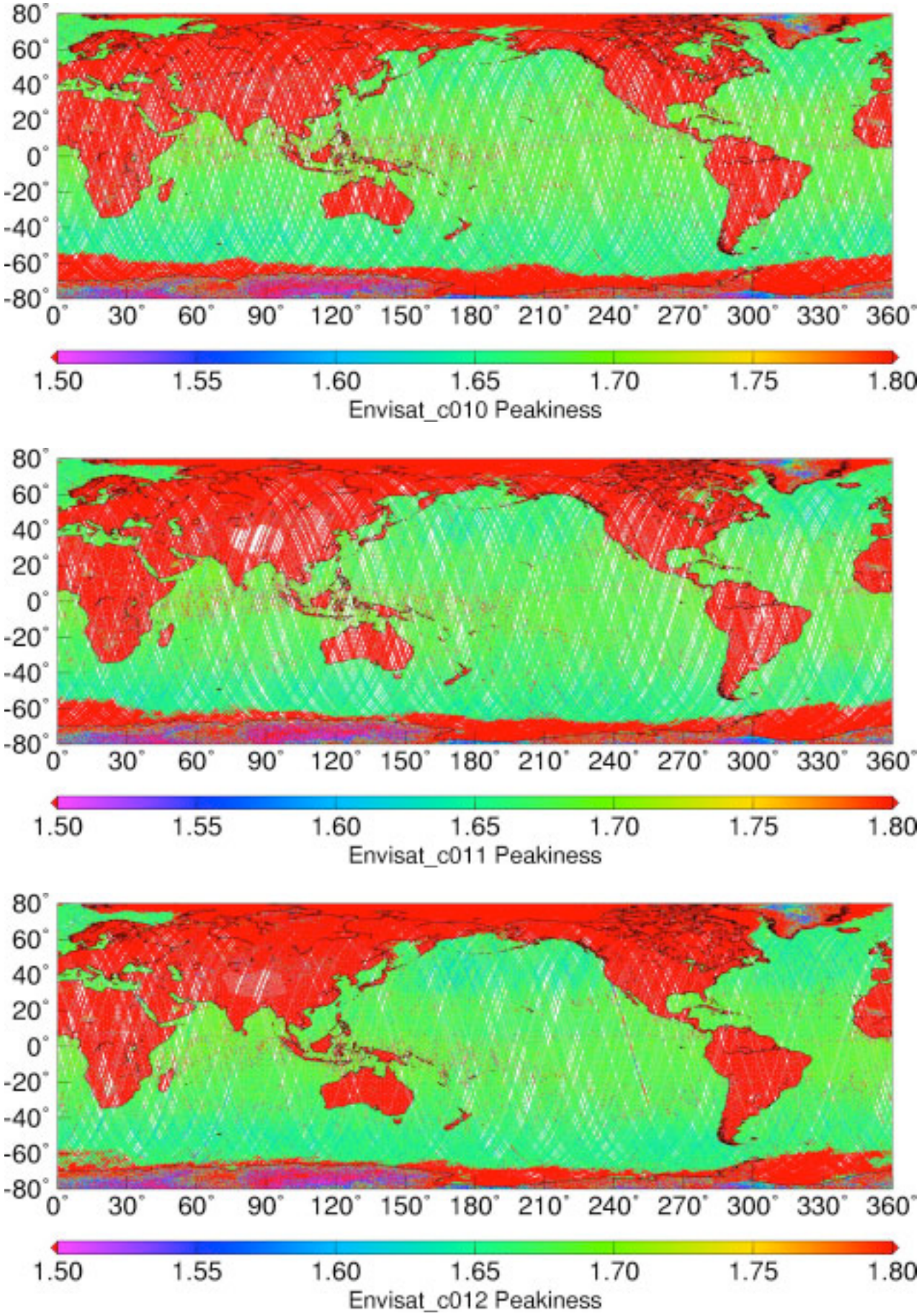

Figure 1. Peakiness distribution for Envisat cycles 10-12.

Although some rain-contaminated values are likely to be edited out by peakiness (note the presence of red dots in the moist equatorial regions in Figure 1) a separate rain flag is desirable, based on the differential attenuation of the dual-frequency altimeter backscatter. The original formulation in the GDRs was based on theoretical considerations and appears to have the correct overall form, but the relationship between Ku-band and S-band backscatter is biased. The current algorithm also has a dependency on liquid water vapor, so that in the absence of MWR data the rain flag bit is set. Figure 2 illustrates the problems with the present rain flag, as well as the radiometer land flag, which are both set in the absence of MWR data. The end user can check for the default value in the MWR wet field to determine the lack of radiometer measurements; these flags should be reserved for data flagged when the rain flag is properly calculated, or when extant radiometer data indicate the values are corrupted by land.

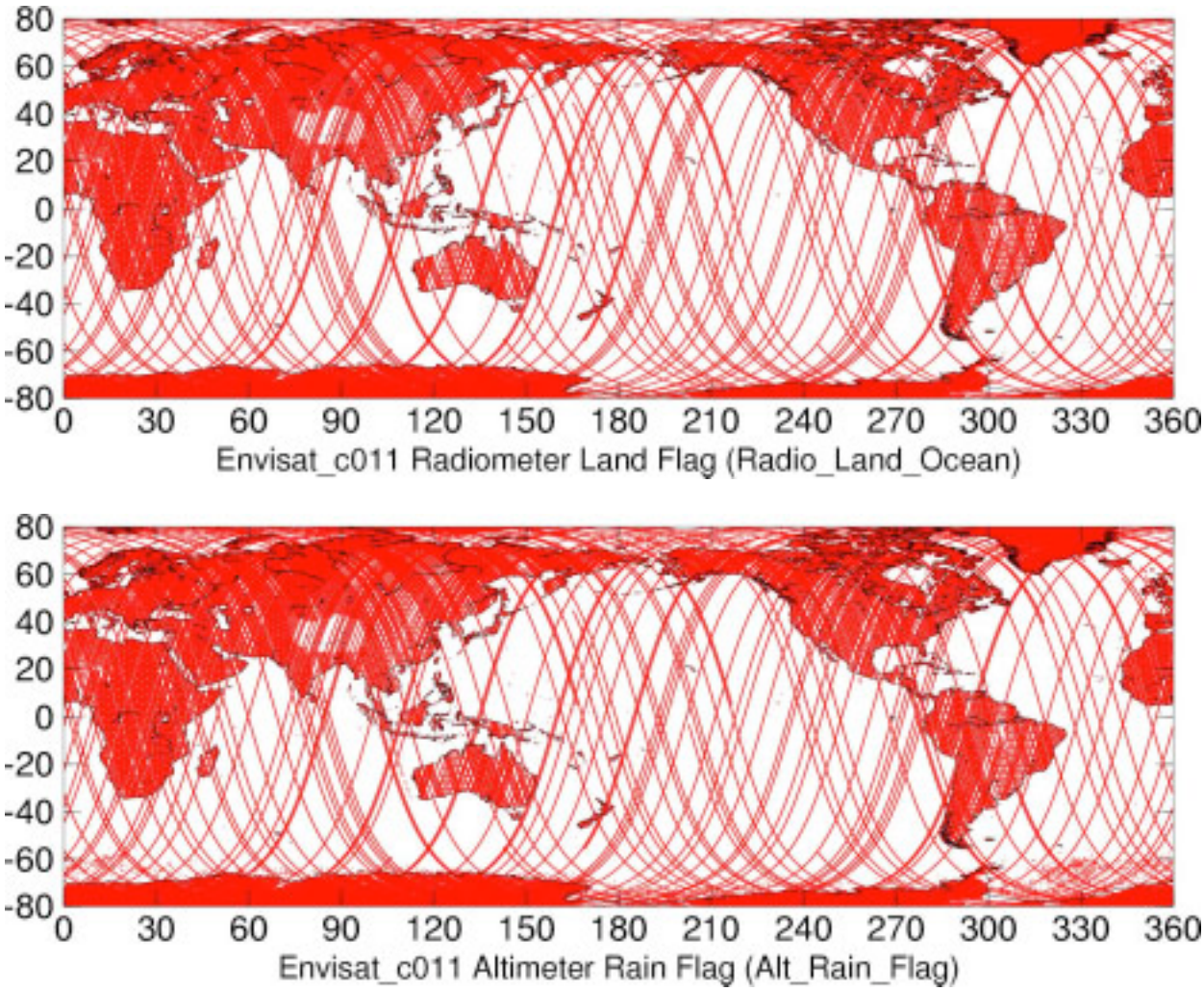

Figure 2. Radiometer-Land and Altimeter-Rain flags for Envisat cycle 11.

A revised altimeter rain flag has been proposed by G. Quartly and J. Tournadre (available in the final CCVT reports website: http://styx.esrin.esa.it:8060/reports) utilizing a small set of preliminary Envisat GDR data. The mean relationship of the difference in backscatter at Ku-band vs. S-band is given in a lookup table, as a function of S-band backscatter (after removing the liquid water attenuation correction to sigma-0). The preliminary estimate of this form is shown in Figure 3.

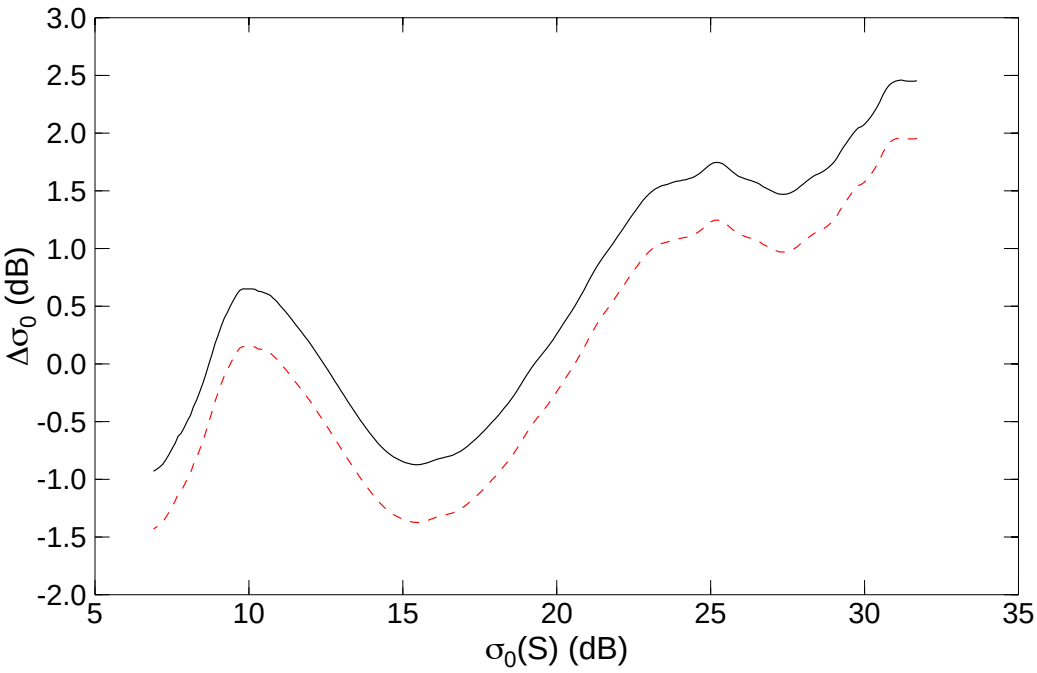

Figure 3. Interim rain flag algorithm from backscatter attenuation.

We utilized their recommendation to flag any data where the difference in backscatter was more than 0.5 dB below the mean curve (as shown by the dotted red line). In this implementation the radiometer information was not utilized at all, though the CCVT recommends that a combination of backscatter attenuation and liquid water content or brightness temperatures ultimately be used in the final rain flag algorithm. The results of flagging data based on backscatter attenuation alone is illustrated for cycle 11 in Figure 4.

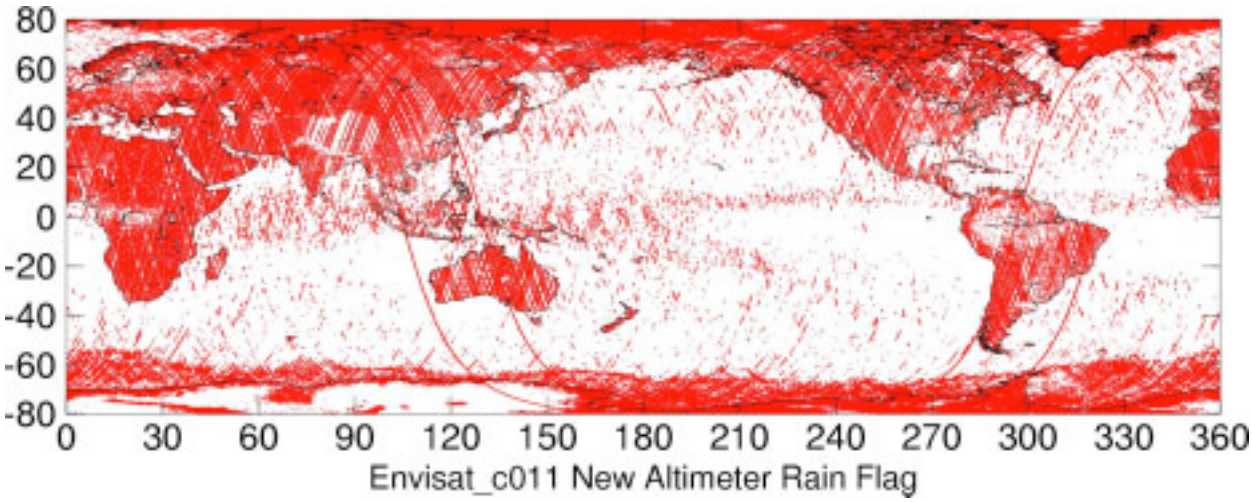

Figure 4. Edited data for Envisat cycle 11 using new rain flag.

Clearly the interim rain flag that we've used is not affected by lack of MWR data, and does a much better job of rejecting points likely to be corrupted by rain, particularly in the tropics.

The remaining flag bit editing that we performed is illustrated in Figure 5 for cycle 11: hardware status (MCD bits 0, 1, or 2); range quality (MCD bits 5 or 17); and backscatter quality (MCD bit 4). These flags have very similar spatial distributions and are primarily removing suspect data over land. Lastly we check the altimeter surface type for continental ice (type=2).

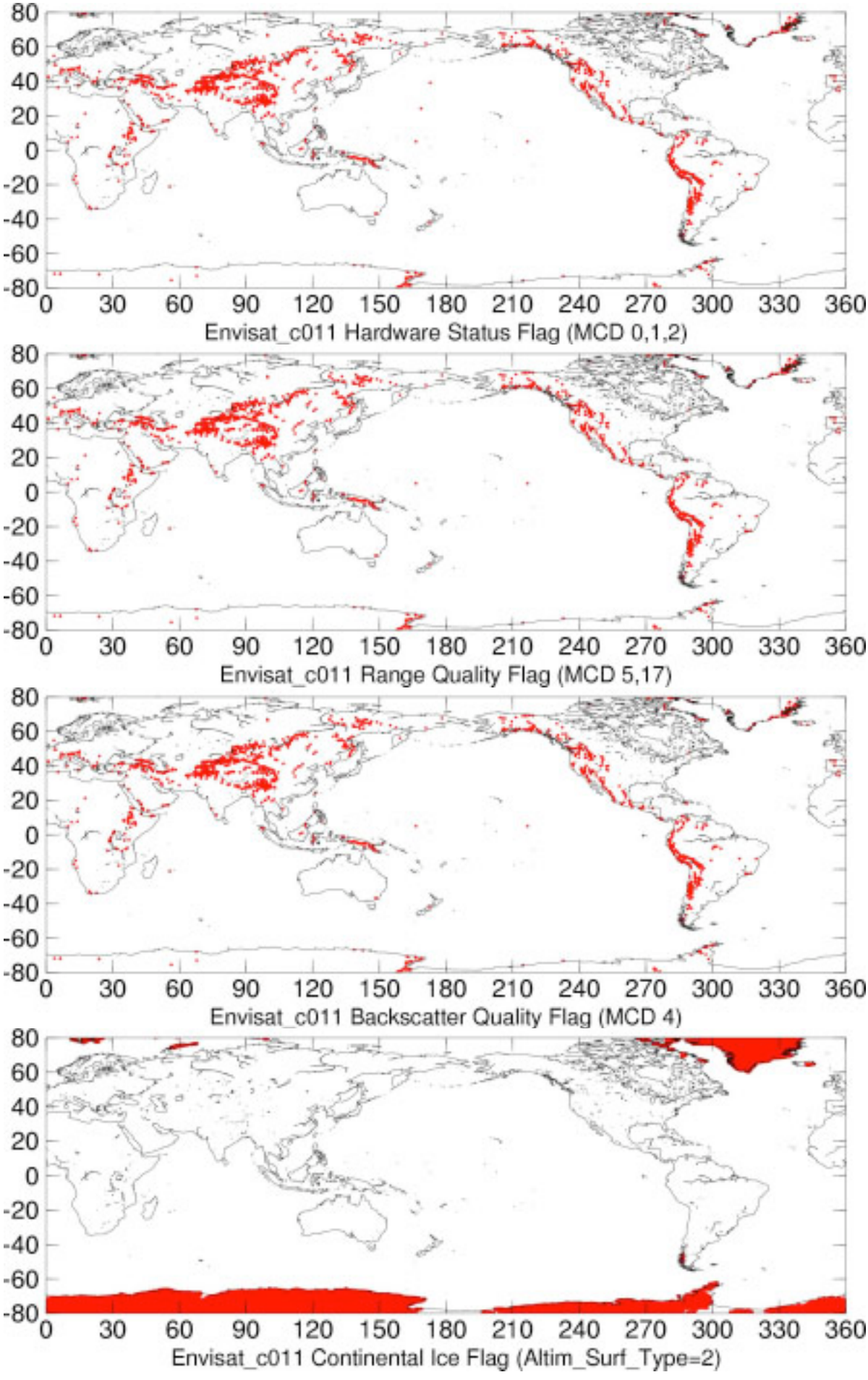

Figure 5. Additional flag bit editing for Envisat cycle 11.

Based on our experience looking at the various edit criteria for the Envisat dataset, we make the following recommendations to the CCVT:

1. do *not* set the radiometer land flag or altimeter rain flag due to missing radiometer data;
2. revise the rain flag algorithm, based on the new backscatter attenuation relationship;
3. explore the possibility of a rain probability index value vs. a simple rain flag bit;
4. incorporate radiometer data in the new rain algorithm where possible; use a flag to indicate if the rain flag is based on backscatter attenuation alone or on backscatter and radiometry;
5. include the peakiness parameter in FDMAR and IMAR products for sea-ice editing.

3. Significant Wave Height

Figure 6 shows the global distribution of Significant Wave Height measured by Envisat for cycles 10-12 and Figure 7 shows the difference in SWH between Envisat and ERS-2. Each of the three panels in Figure 7, as in most of the following difference figures, shows the global distributions of differences between nearly coincident collinear pairs. The top panel is for the pair Envisat cycle 10 and ERS-2 cycle 78; the middle panel for Envisat cycle 11 and ERS-2 cycle 79; the bottom panel for Envisat cycle 12 and ERS-2 cycle 80. In all cases the time delay between the ERS-2 and Envisat measurement is approximately 30 minutes.

Clearly, there are no alarming differences between the wave heights measured by the two altimeters, except for an approximately 20 cm offset. The off-scale differences near the poles (particularly the Antarctic) are measurements contaminated by sea ice.

The scattergram in Figure 8 compares the wave heights measured by ERS-2 (horizontal coordinate) with those measured by Envisat (vertical coordinate) during the three collinear cycles. Along each of the coordinate axes the one-dimensional histogram of the data is indicated by a thick black curve. The colors indicate the frequency of occurrence on a logarithmic scale. The numbers on the side of the graph indicate some important statistics of the data and their mutual regressions. From top to bottom, these are: number of collocated points, the mean and standard deviation of the respective measurements (denoted x and y), the regression parameters (slope and intercept) and the rms-of-fit for the regression of the y-coordinate against the x-coordinate and *visa versa,* and finally the regression coefficient.

This plot shows that there is a 21.9 cm bias in the ERS-2 wave heights with respect to the Envisat data. The ERS-2 wave height distribution is clearly clipped to zero at low wave heights. It is very likely that the ERS-2 wave heights are too low rather than the Envisat wave heights being too high, based on comparisons with in situ ocean buoy data [D. Cotton, pers. comm.]

It is evident from Figure 8 that ERS-2 wave heights are too low by about 22 cm. As a consequence, the low wave heights (say below 22 cm) are all set to zero. This makes it impossible to 'undo' the bias at low wave heights. While at higher wave heights the bias can simply be added to the ERS-2 measurement, all the zero values will become 22 cm wave heights, which is unrealistic. If the sign of the wave height would have been kept, negative ERS-2 wave heights would have been properly mapped to positive values. The constraint to avoid negative wave heights has thus made it impossible to recover proper ERS-2 wave height measurements at wave heights below 22 cm. This is even worse in the case of ERS-1, whose wave heights are even more biased low. Hence another recommendation by the CCVT to the project is to allow signed integer values for quantities such as SWH and backscatter to avoid clipping in the presence of such measurement biases.

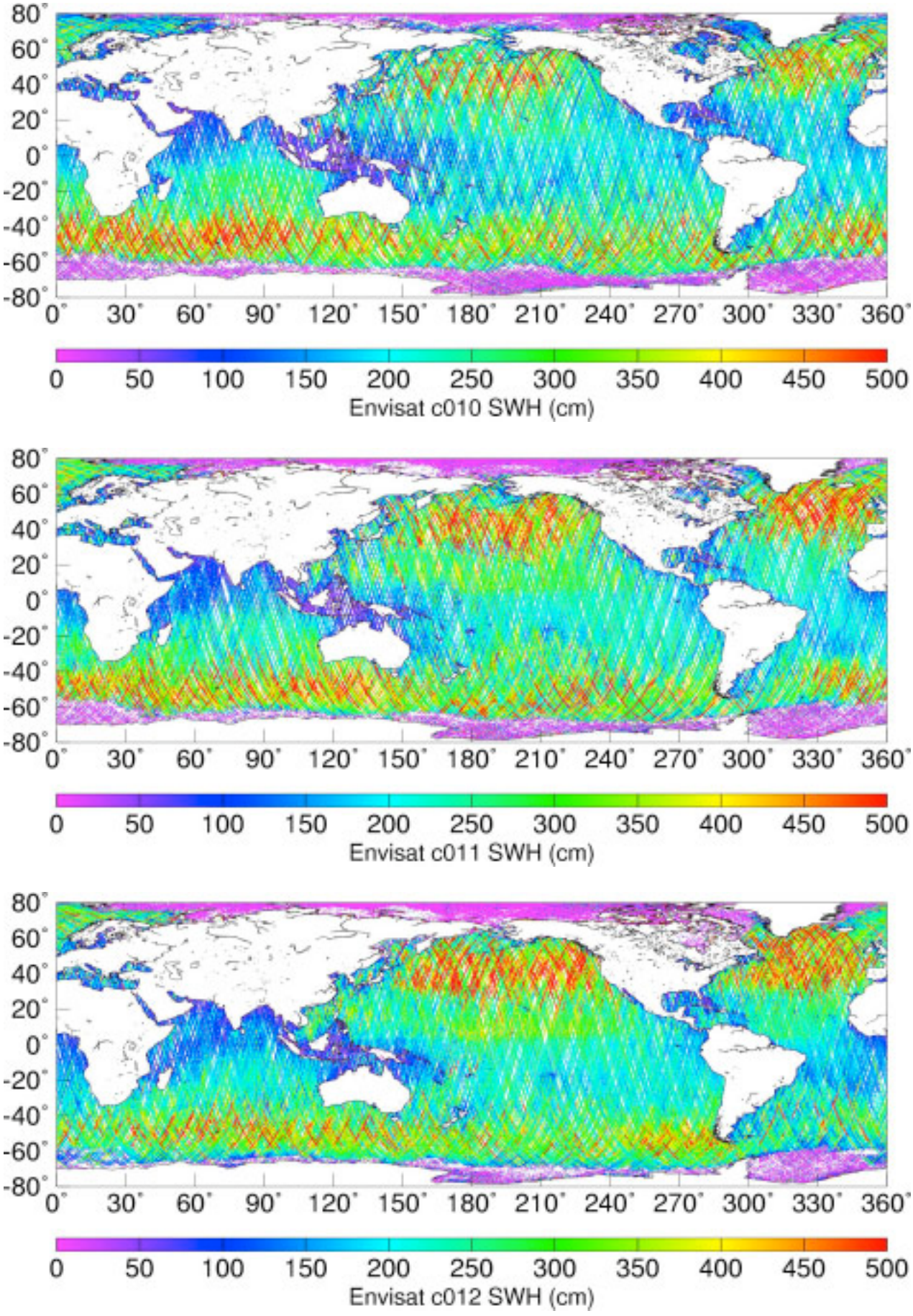

Figure 6. Significant Wave Height for Envisat cycles 10-12.

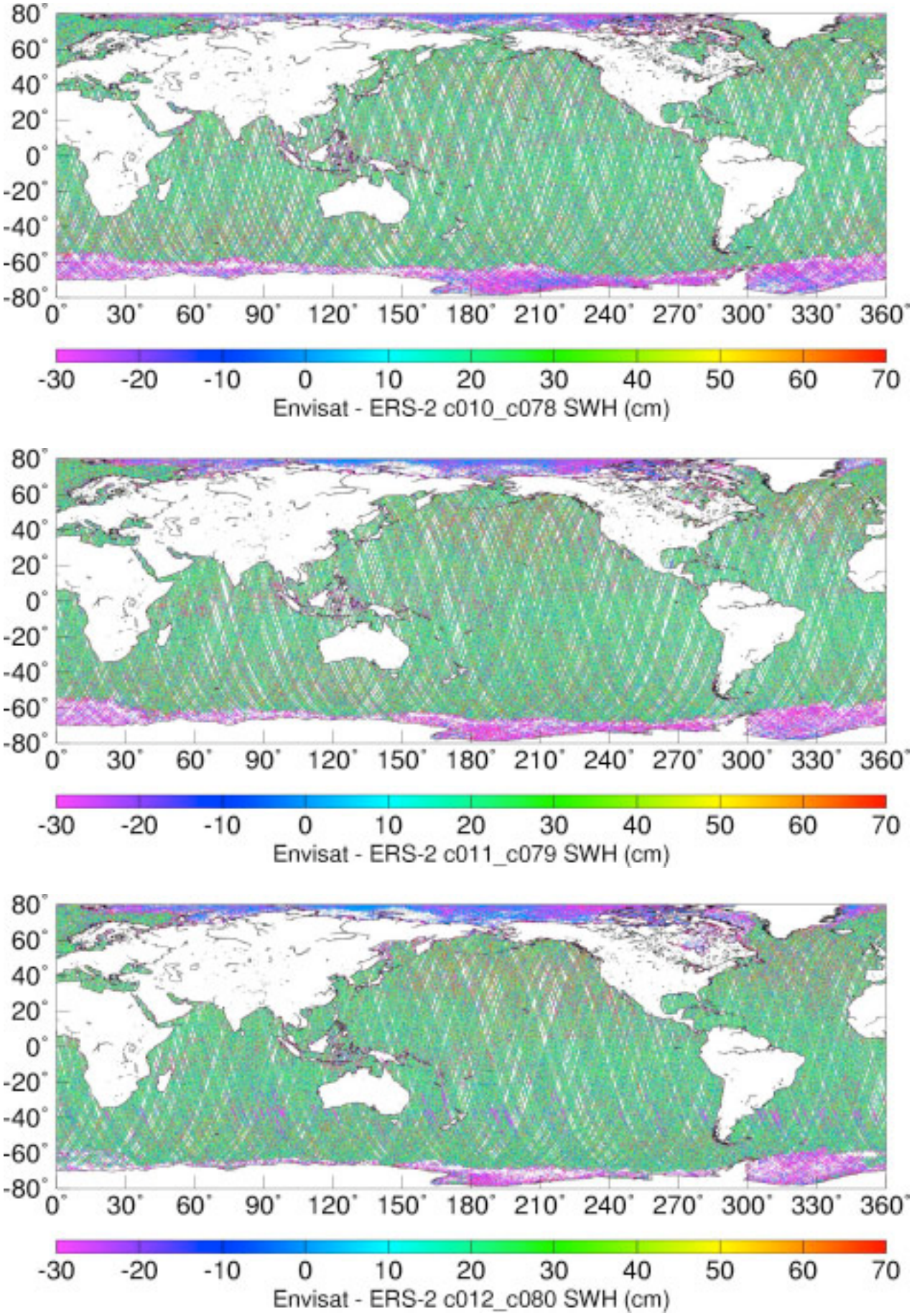

Figure 7. Significant Wave Height differences: Envisat – ERS-2.

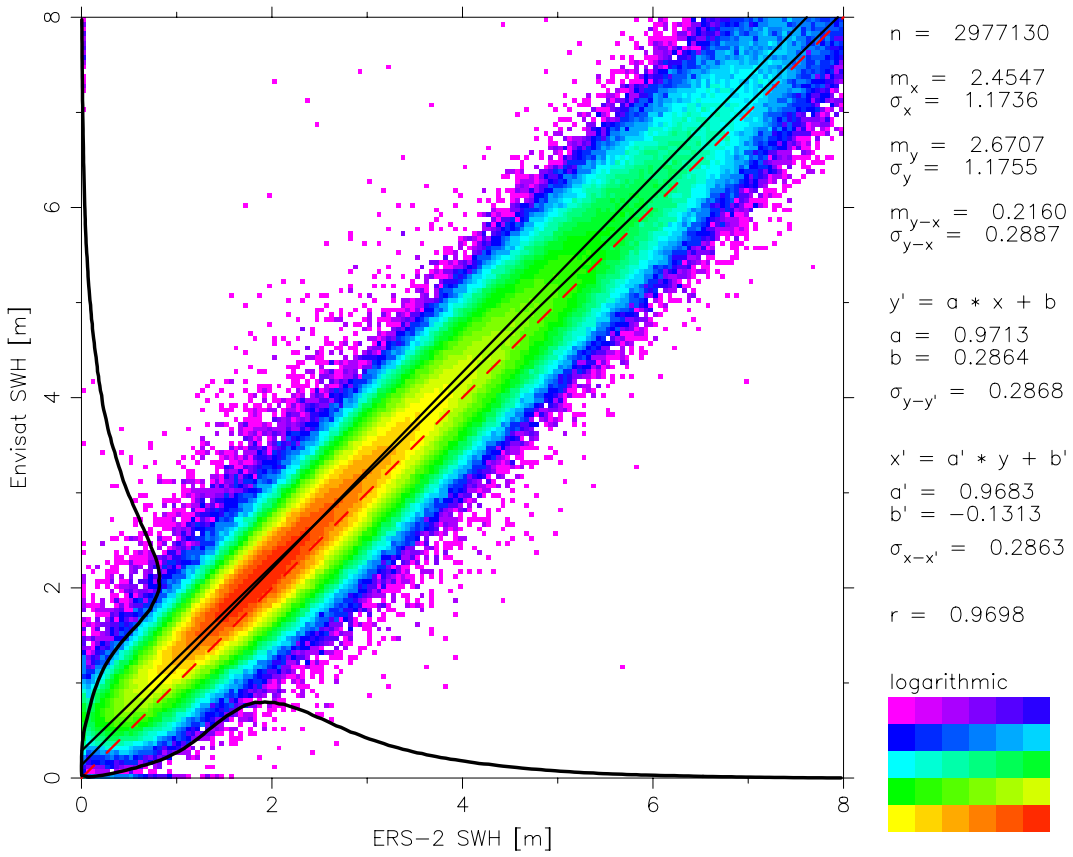

Figure 8. Scattergram of Significant Wave Height: Envisat vs. ERS-2.

4. Backscatter and Wind Speed

Figure 9 and Figure 10 show the global distribution of radar backscatter (σ_0) for Envisat as well as the difference between the backscatter coefficient measured by Envisat and ERS-2. The differences are generally small, except in 'wet' areas around the Tropical Convergence Zone, where Envisat's σ_0 is about 0.5 dB higher. We currently have no explanation for the fact that the cycle 12/80 pair shows scattered large differences also around 40° S. Clearly, the large bias in the Envisat backscatter, reported during earlier CCVT meetings, has been removed.

Figure 11 shows the two-dimensional scattergram of the backscatter as measured by ERS-2 and Envisat. It is evident that the two measurements are very close, with no significant bias or tilt between them. Note that the differences are somewhat larger in the low and high backscatter regimes (high and low winds) compared to the middle regime. Envisat shows a more uniform Gaussian distribution of the backscatter than ERS-2. The ERS-2 measurements seem to be grouped erroneously in about 6 different Gaussian distributions each separated by 1 dB.

The absolute calibration of the backscatter coefficient seems to indicate that the Envisat backscatter is low by about 1 dB. Since all previous altimeters have in some way been calibrated against Geosat, this means that all altimeter backscatter measurements are biased low by that amount. It is important to keep in mind that this bias will have to be taken into account in future developments of algorithms to derive wind speed, wet troposphere delay (from microwave radiometers) and the sea state bias.

This 1 dB bias was not yet added when using the backscatter coefficient in the current implementation of the algorithm for the microwave radiometer wet troposphere delay. This will have to be accounted for in future Envisat GDR releases.

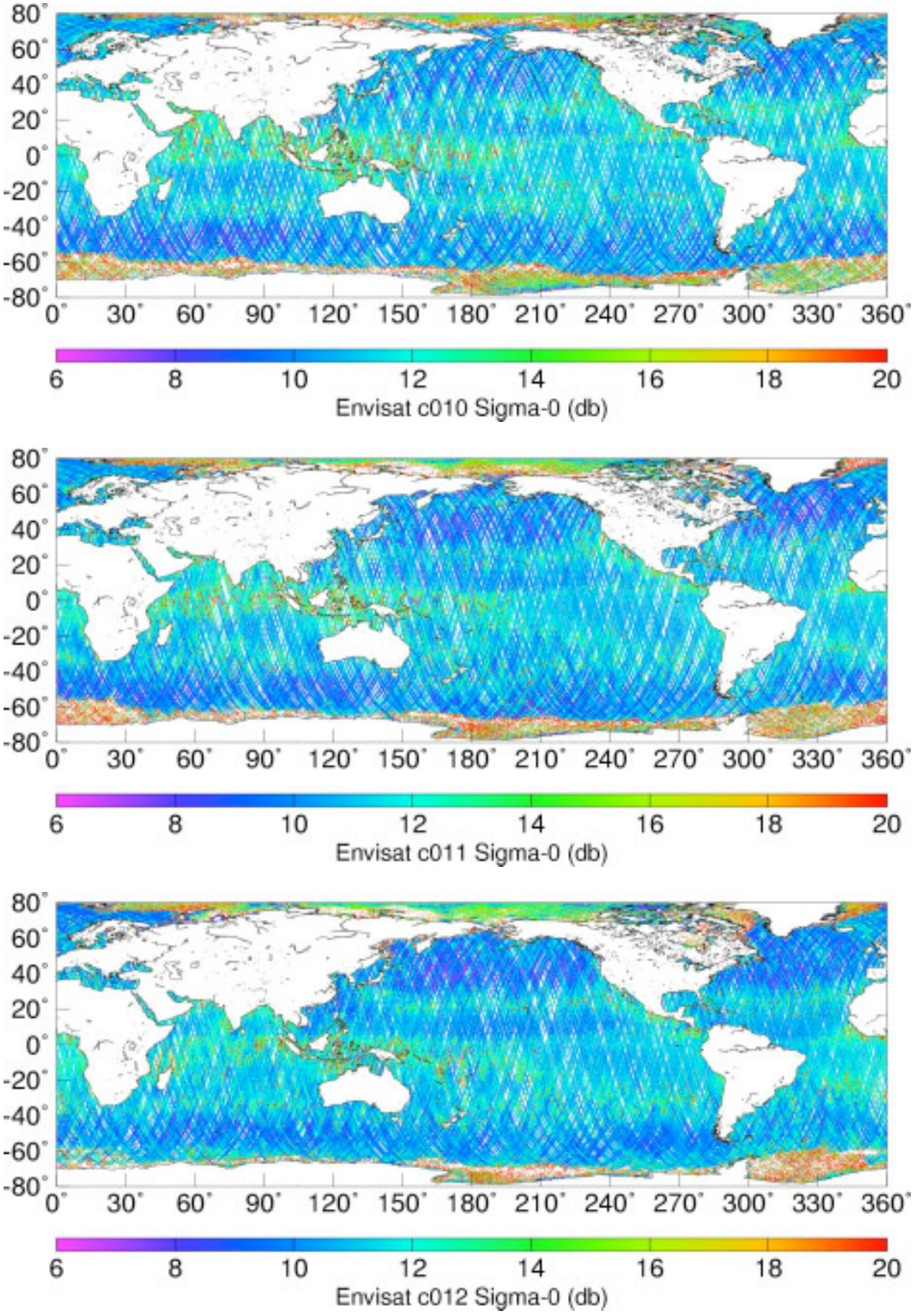

Figure 9. Backscatter coefficient for Envisat cycles 10-12.

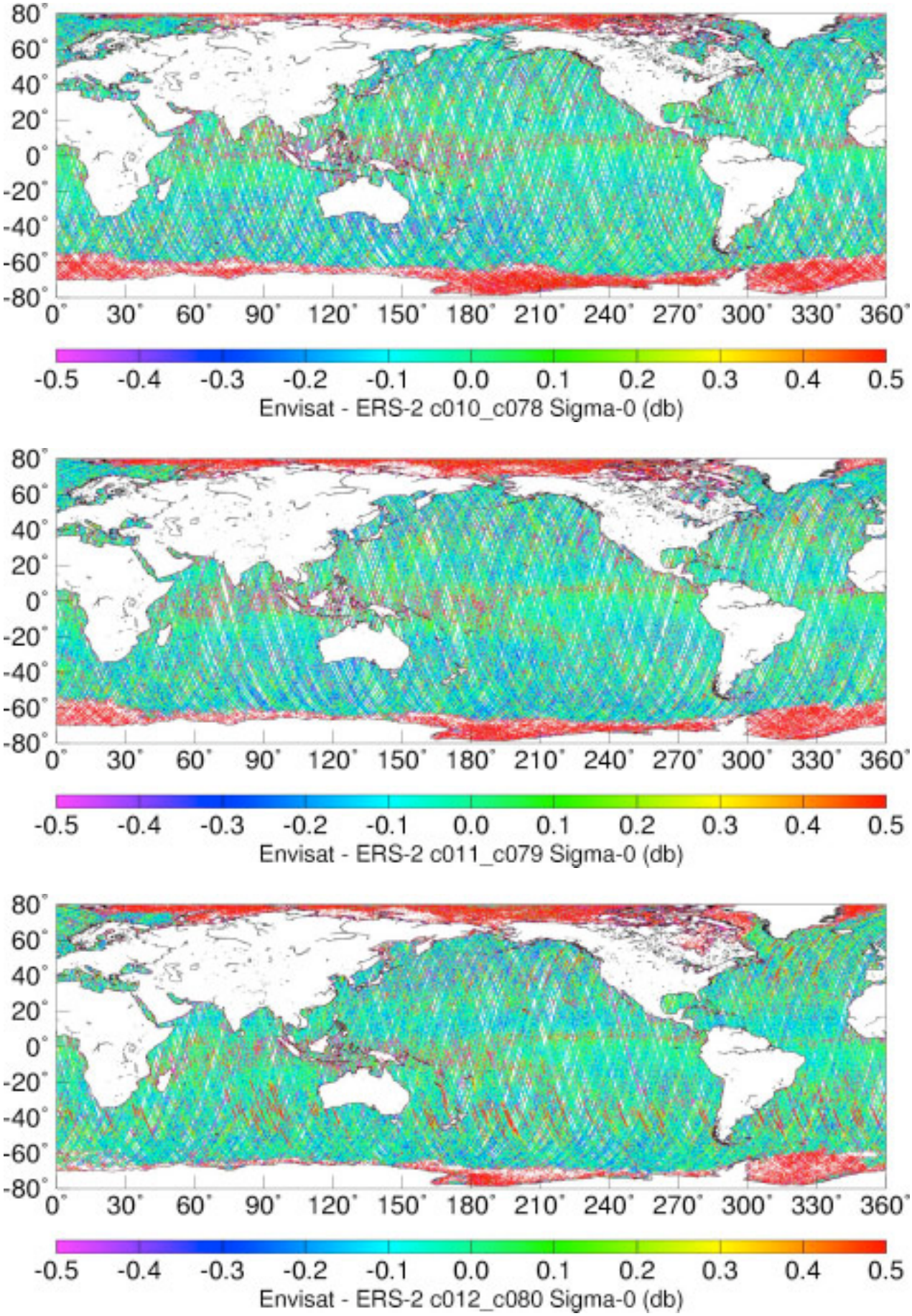

Figure 10. Backscatter coefficient differences: Envisat – ERS-2.

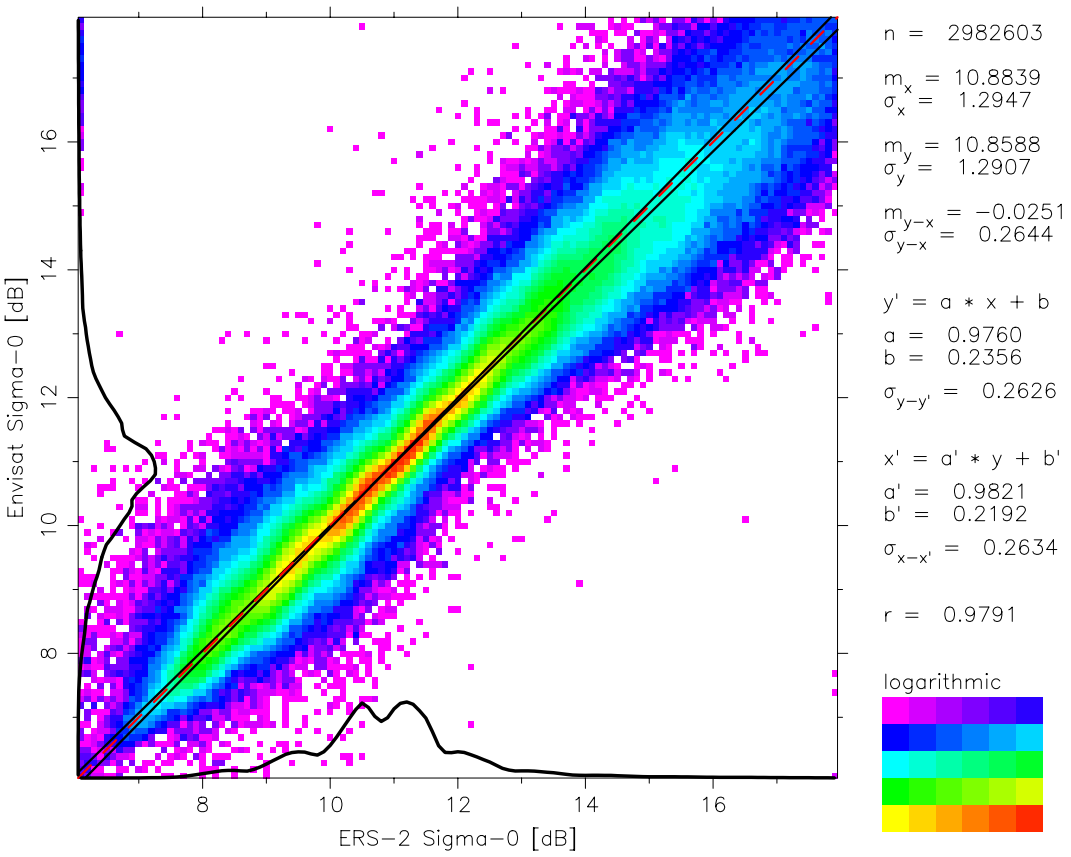

Figure 11. Scattergram of backscatter coefficient: Envisat vs. ERS-2.

5. Environmental Corrections

To validate the various environmental corrections to range we compare the equivalent correction for ERS-2 vs. Envisat. Both the dry troposphere path delay and the inverse barometer (IB) sea surface effect are based on surface atmospheric pressure values coming from the ECMWF meteorological models. In principle the 30-minute difference in over flight time of the two satellites should be the only difference in interpolating the 6-hourly model grids, since both datasets are utilizing the same ECMWF model. It came to our attention at the final CCVT meeting in March 2003, that there could be differences in the handling of the ECMWF data, related to spectral (Gaussian) vs. physical (Cartesian) grids for Envisat and ERS-2 respectively. As we show below there is little impact on the dry troposphere correction, but an unexpectedly large difference in the model wet troposphere correction that may be due to this use of different model grids.

The global distribution of the dry troposphere corrections for Envisat are shown in Figure 12, followed by the distributions of differences between the Envisat and ERS-2 dry troposphere corrections in Figure 13.

The differences between the dry correction for Envisat and ERS-2 are indeed small, on the order of a few mm. There are four strange patches (around 50°, 140°, 230° and 320° longitude) where the correction differences are systematically different by more than 1 mm. Although these differences are small and may be the result of the 30-minute time difference, they should be investigated.

The inverse barometer correction scales as about 4.5 times the dry troposphere correction, and hence the difference plots for the inverse barometer (not shown) are in the range of ±14 mm. The global distribution of the inverse barometer correction (after removing the global over-ocean mean, rather than a fixed 1013.3 mbar) is shown in Figure 14.

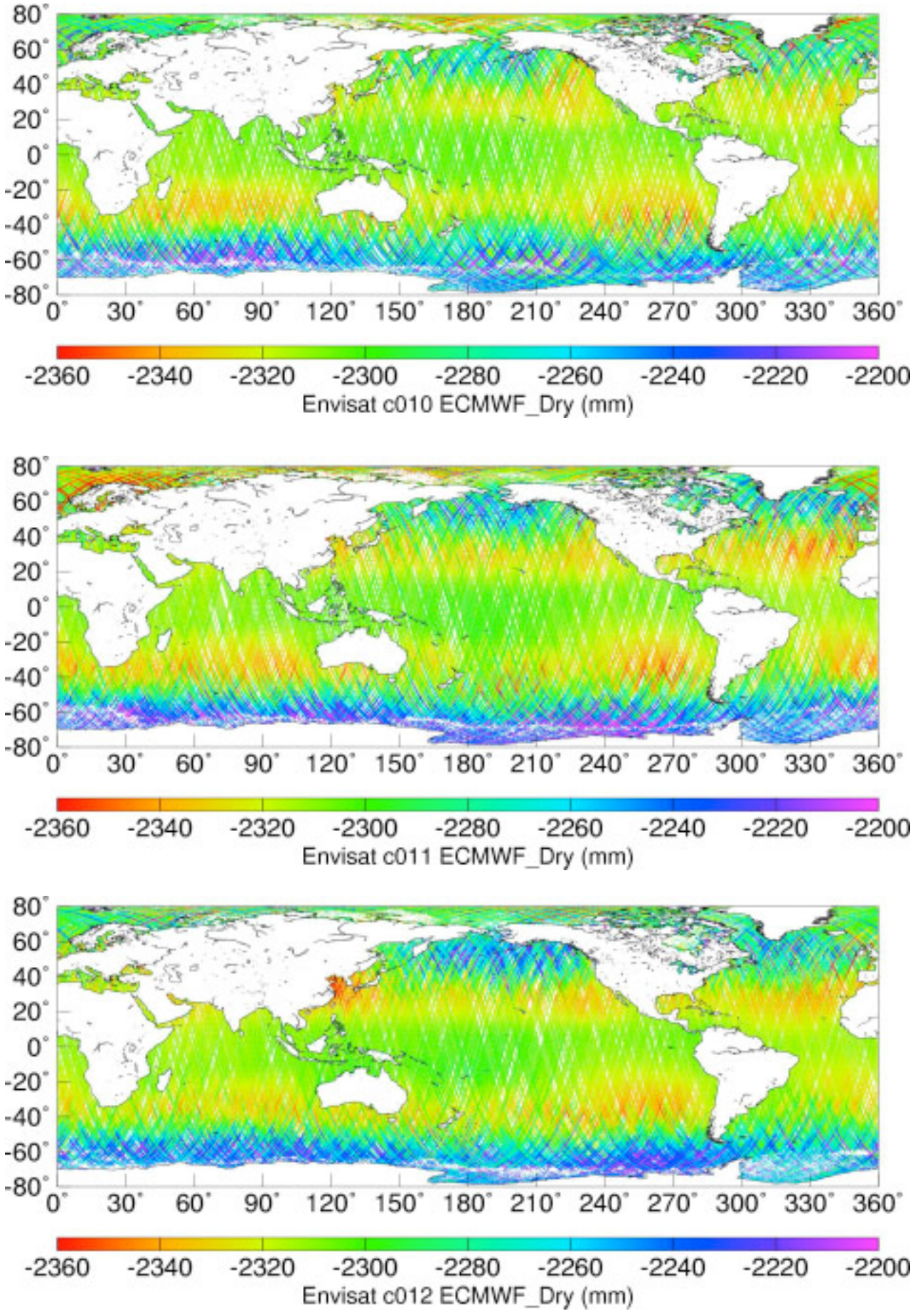

Figure 12. ECMWF dry troposphere correction for Envisat cycles 10-12.

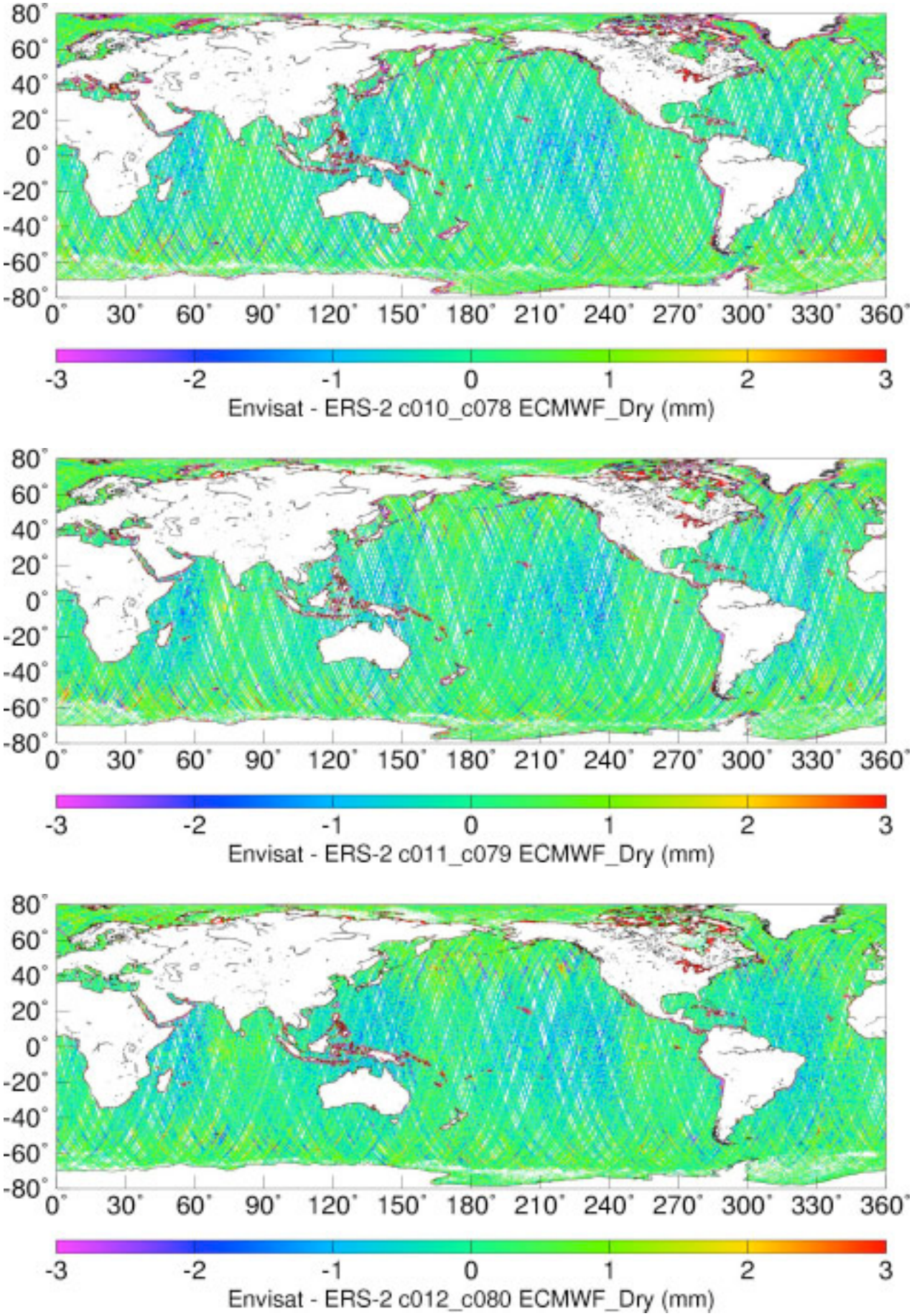

Figure 13. ECMWF dry troposphere differences: Envisat - ERS-2.

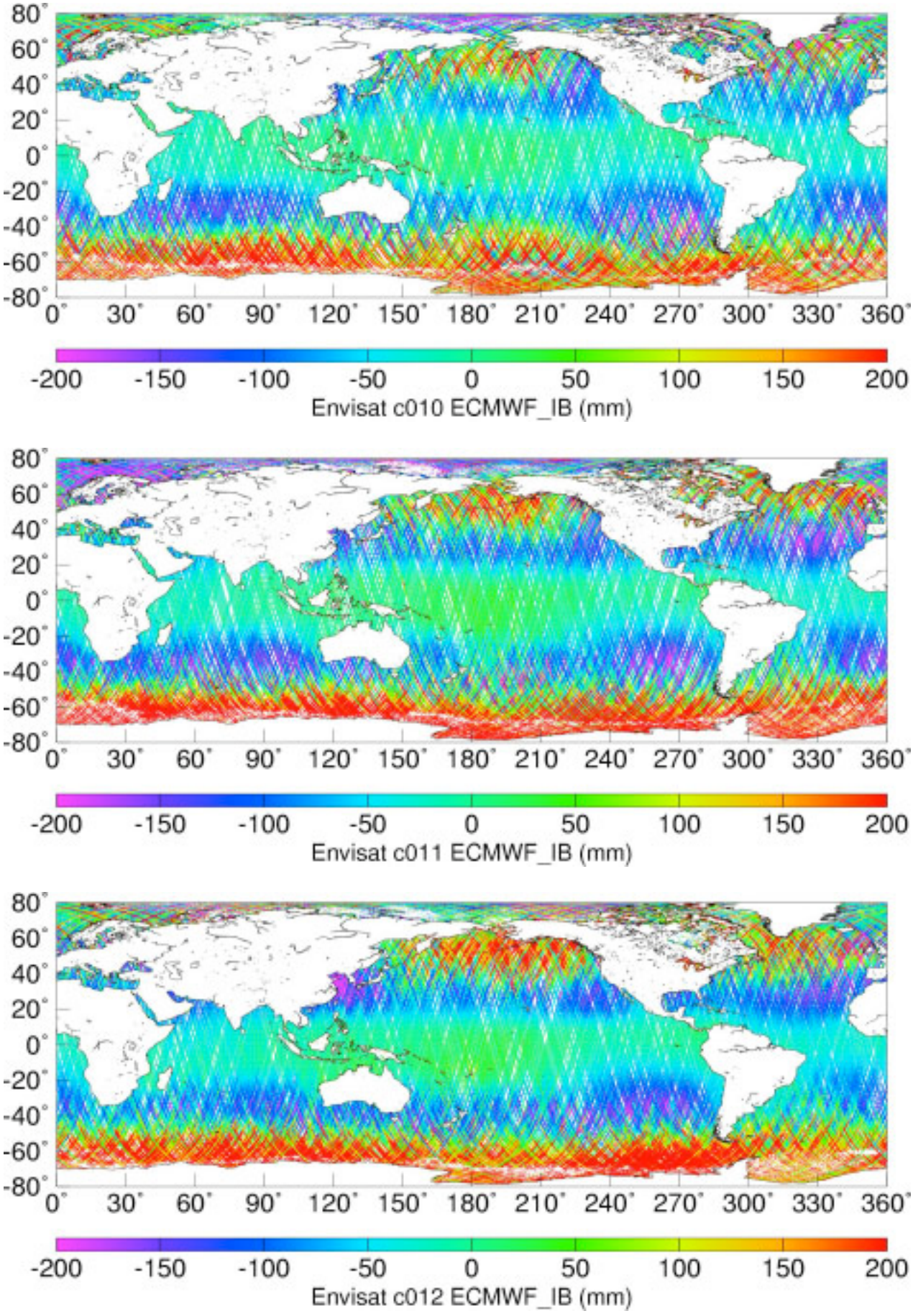

Figure 14. Inverse barometer correction for Envisat cycles 10-12.

It is important that the user is aware of the reference pressure used in the IB correction. In ERS-2 the IB correction is based on the nominal mean reference sea level pressure of 1013.3 mbar (exactly one 'atmosphere'), which is in fact about 3 mbar higher than the actual temporal and global mean sea level pressure (over oceans). For Envisat the reference pressure is the actual global mean sea level pressure (over oceans), which varies by 1-2 millibar around the 1010 mbar level. This means that when the ERS-2 IB correction is not computed in the same way, an apparent 3 cm bias with a 1-2 cm seasonal oscillation is introduced.

The scattergram in Figure 15 also illustrates the small differences between the Envisat and ERS-2 dry corrections. Again, due to the simple scaling argument between the dry and inverse barometer corrections we only present the scattergram for the dry correction. This plot shows no systematic differences between the values recorded on the Envisat and ERS-2 products. It seems as though the Envisat values are noisier. The cause of this should be investigated.

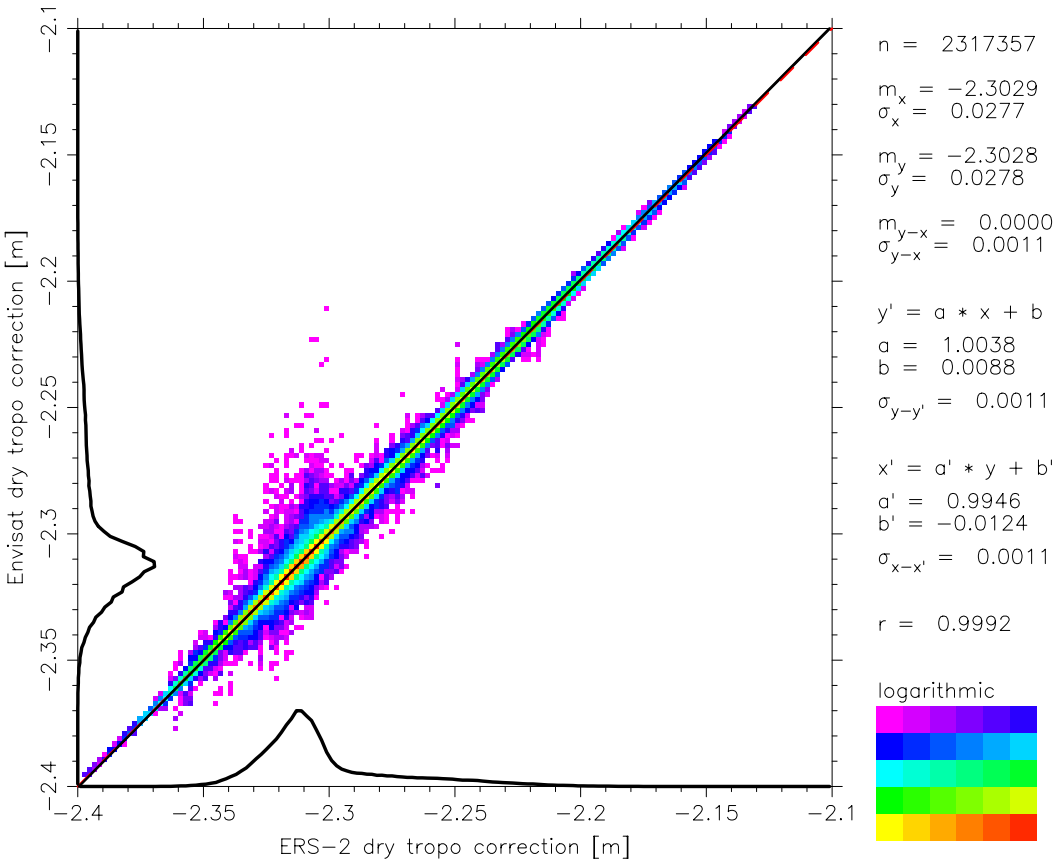

Figure 15. Scattergram of ECMWF dry correction: Envisat vs. ERS-2.

5.1. ECMWF Model Wet Troposphere Correction

As in the previous section, we show both the global distribution of the ECMWF wet troposphere correction reported on the Envisat GDRs (Figure 16), as well as the distribution of the difference with the ERS-2 OPR values (Figure 17). The latter plot clearly reveals that in the wet regions the Envisat correction is significantly smaller (hence dryer) than the ERS-2 correction.

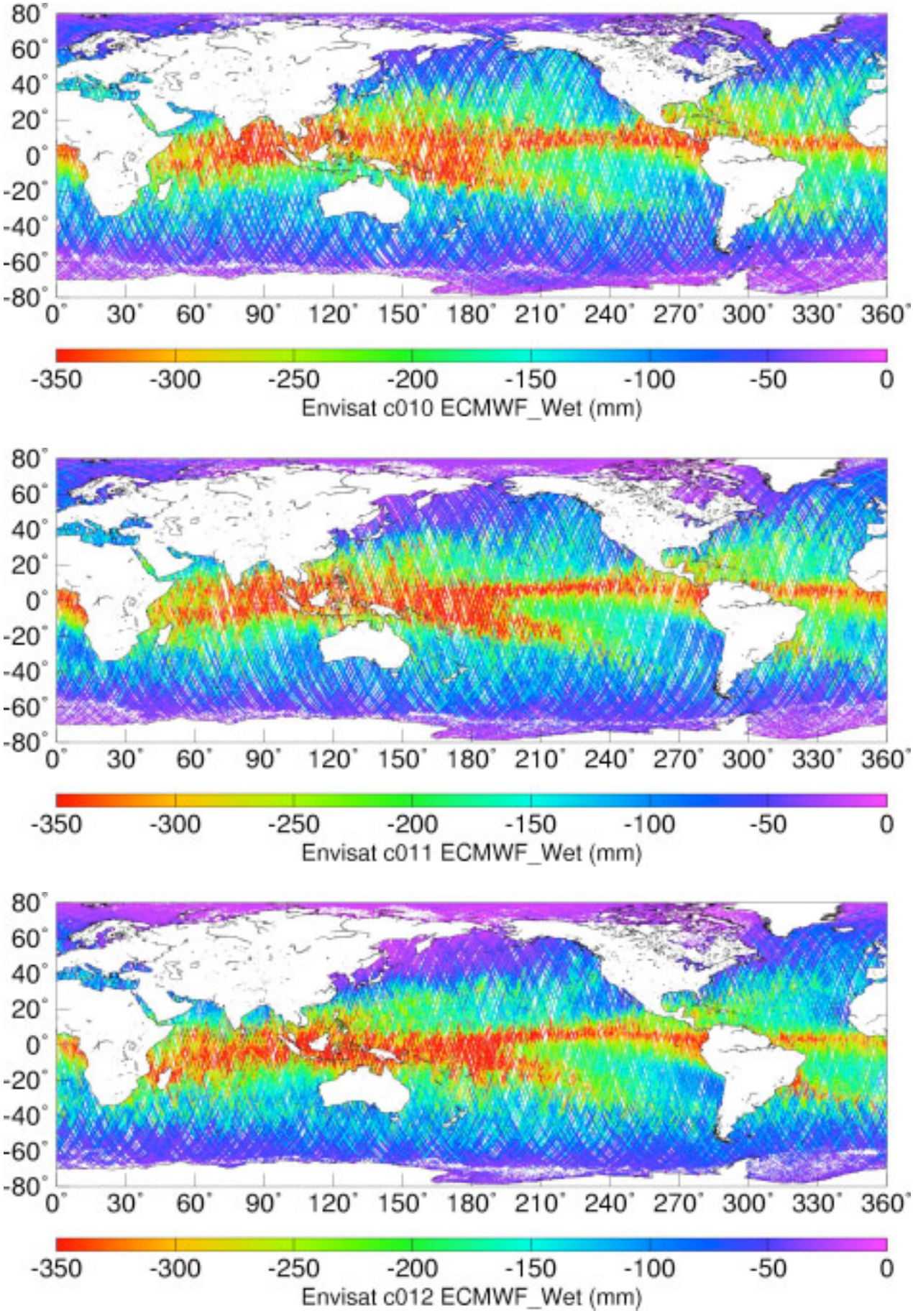

Figure 16. ECMWF wet troposphere correction for Envisat cycles 10-12.

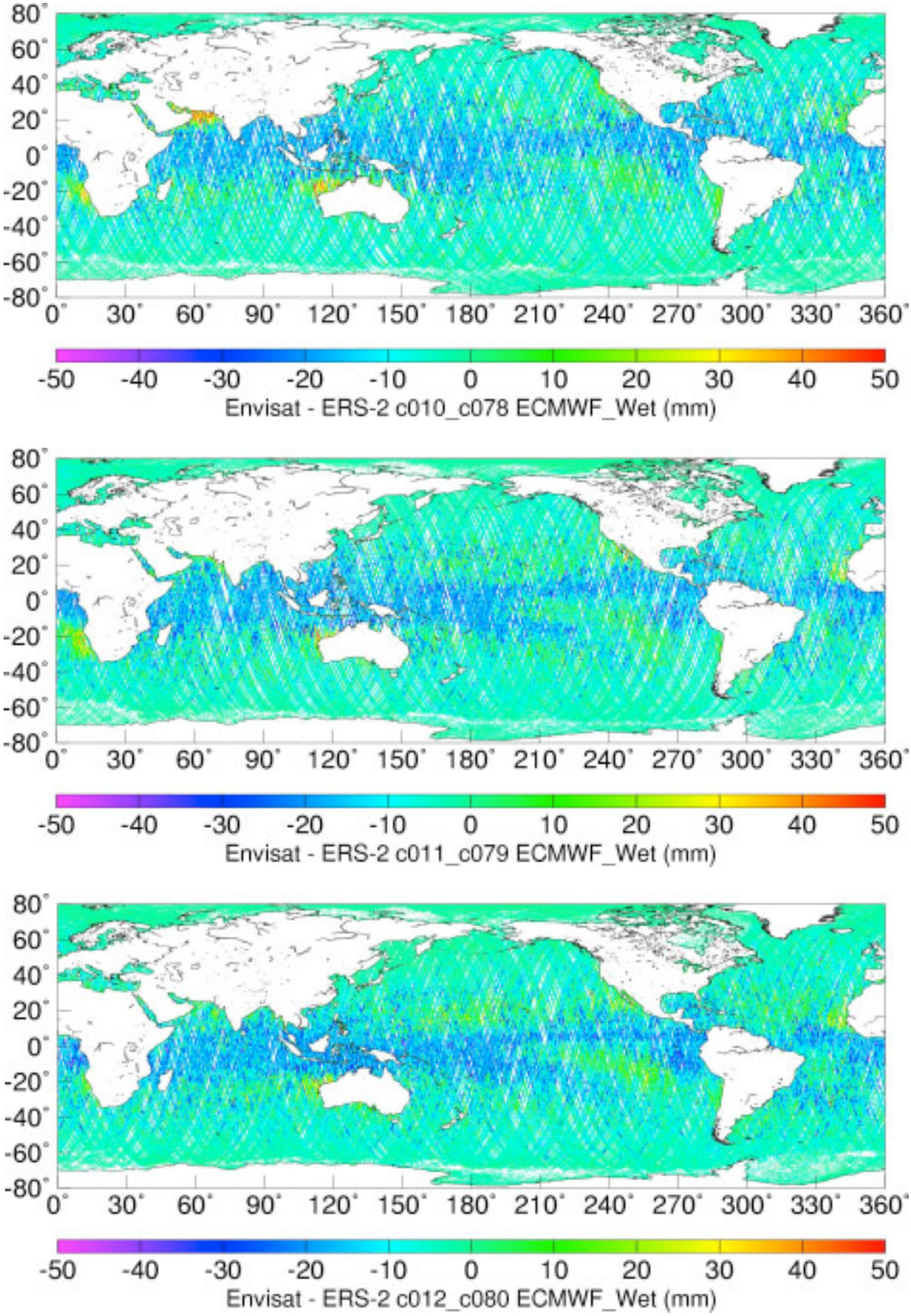

Figure 17. ECMWF wet troposphere differences: Envisat - ERS-2.

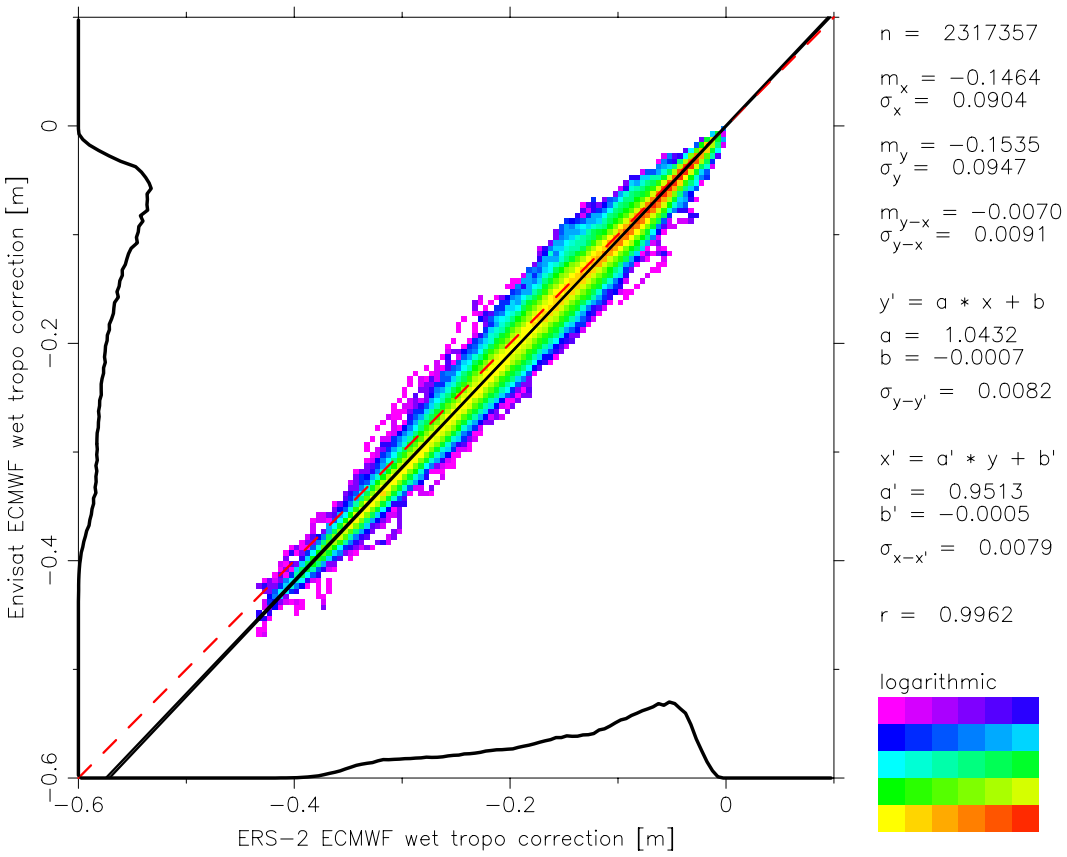

Figure 18. Scattergram of ECMWF wet correction: Envisat vs. ERS-2.

When the two model corrections are compared in the form of a scattergram (Figure 18), it becomes clear that the Envisat values are systematically underestimating the wet troposphere delay by about 4.6%. It has been suggested that this is due to the way the correction is evaluated (using a spectral rather than Cartesian representation of the atmosphere). However, this should not introduce systematic differences. The cause of the difference in scale of the wet troposphere correction should be investigated!

5.2. Radiometer wet troposphere correction

On all altimetry missions since Geosat a passive microwave radiometer (MWR) is the primary means for measuring coincident wet troposphere delays at nadir to correct the range. Here we compare the MWR wet troposphere values on Envisat vs. ERS-2 as we did the model wet corrections in the previous section. Since the radiometer will be independently calibrated, we do not use the MWR wet correction in our range calibration below. However, we do want to assess the quality of these measurements in conjunction with the model wet corrections. Figure 19 shows the global distribution of the Envisat MWR wet troposphere correction, and Figure 20 the differences between the MWR wets on Envisat compared to ERS-2.

The global distribution plots indicate that Envisat's MWR is measuring wetter (larger negative) values in the tropics compared to ERS-2 by some 2-3 cm, but is measuring dryer (smaller negative correction) relative to ERS-2 in mid-latitudes and polar regions, again by some 2-3 cm. This is confirmed by the scattergram in Figure 21, where we see that the best fit line (in black) is tilted relative to the 45° line (red-dashed line) such that high water vapor regions are too wet according to Envisat and low water vapor regions are too dry relative to ERS-2. In fact in the dry regime the Envisat MWR is actually reporting positive, vs. small negative, corrections.

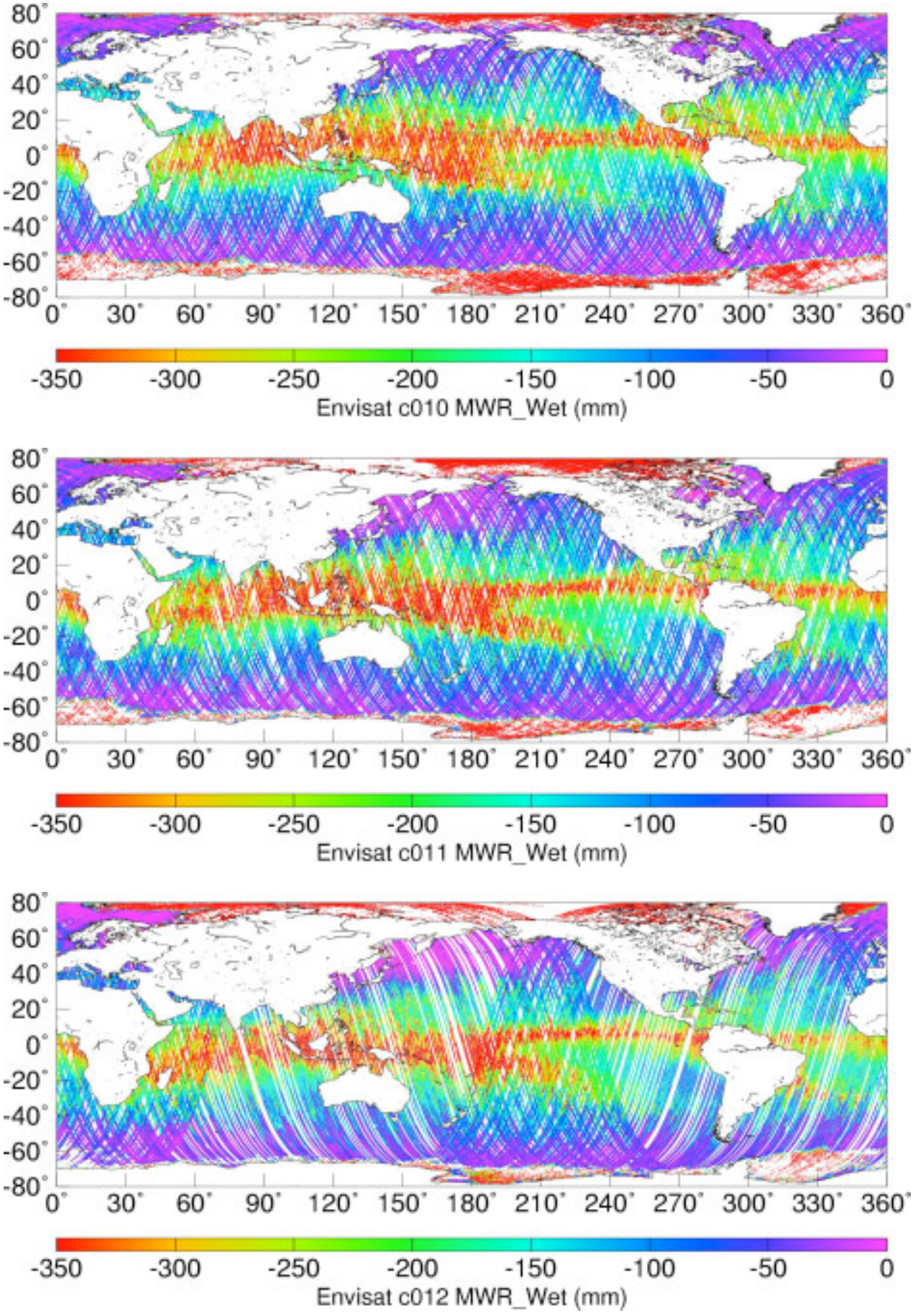

Figure 19. Microwave radiometer wet troposphere correction for Envisat cycles 10-12.

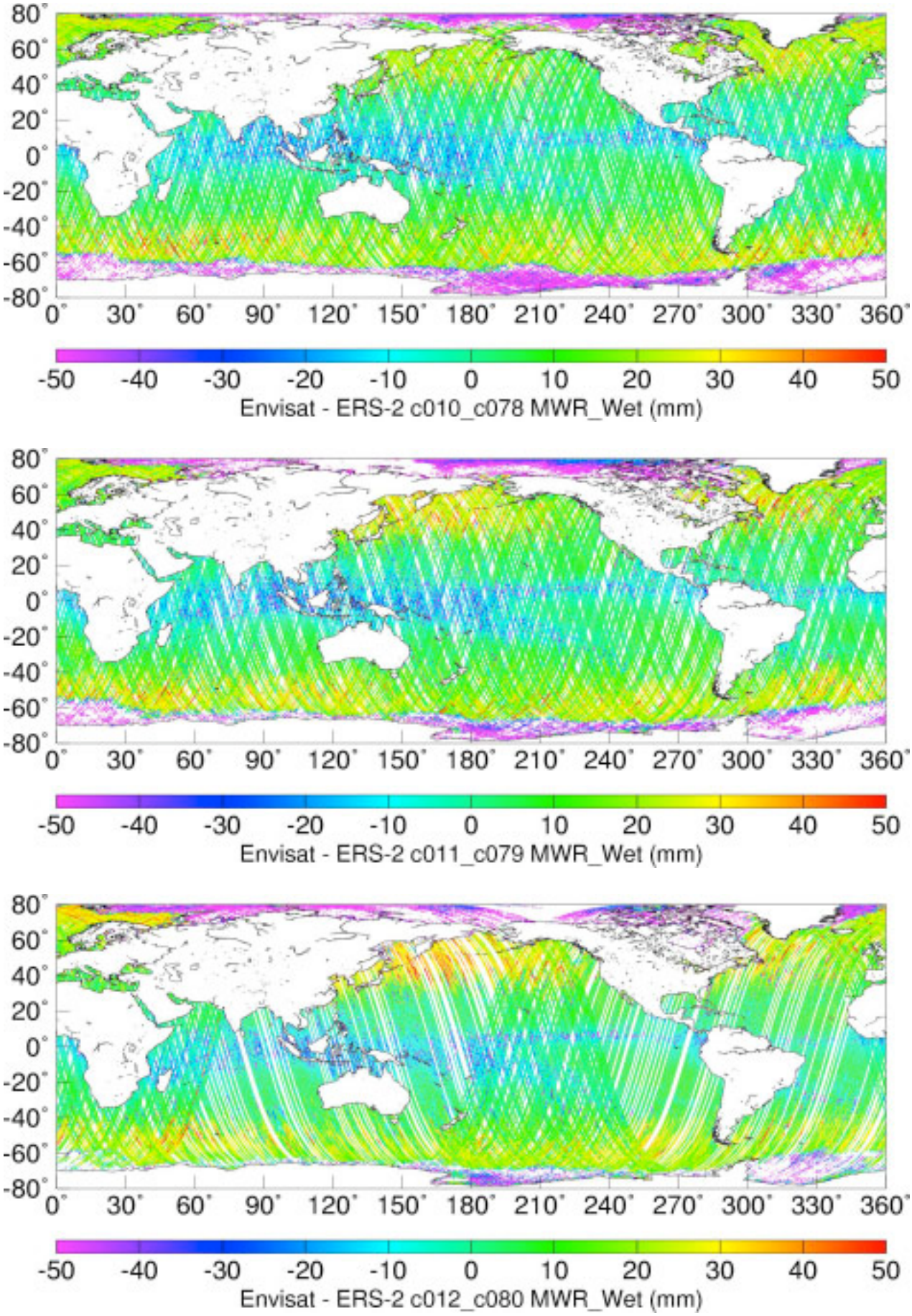

Figure 20. MWR wet troposphere differences: Envisat - ERS-2.

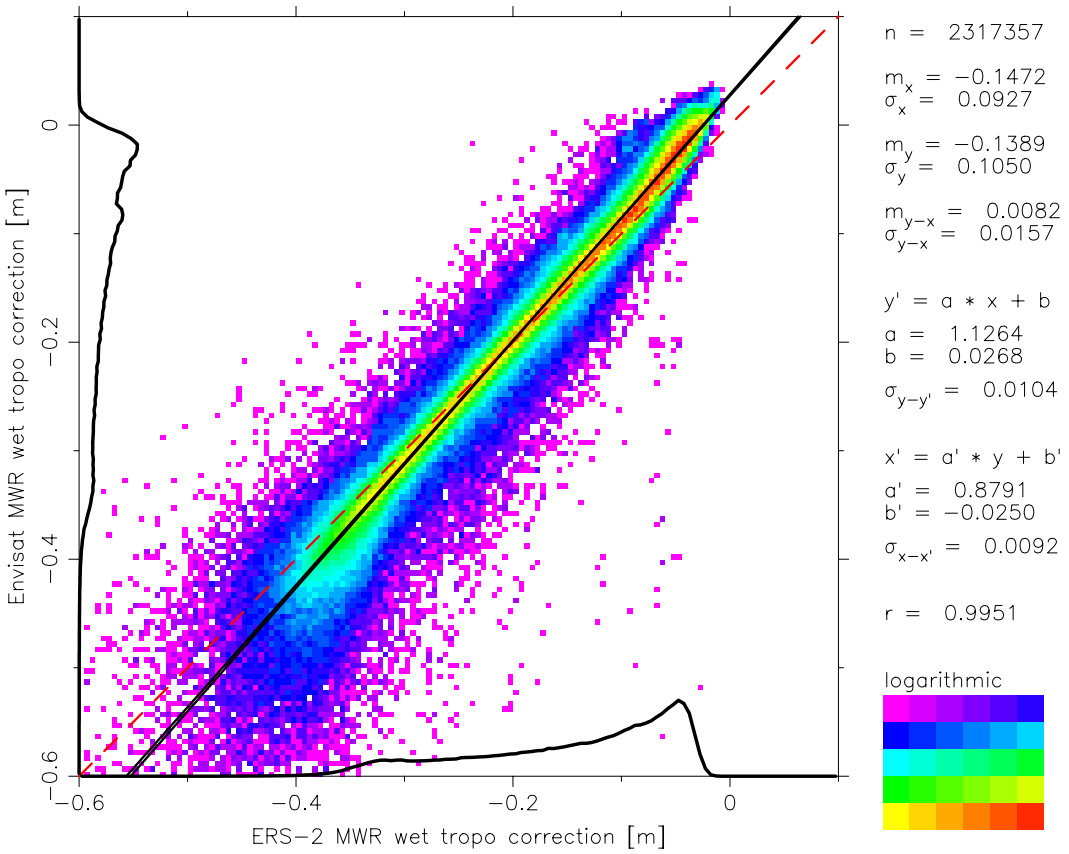

Figure 21. Scattergram of MWR wet troposphere: Envisat vs. ERS-2.

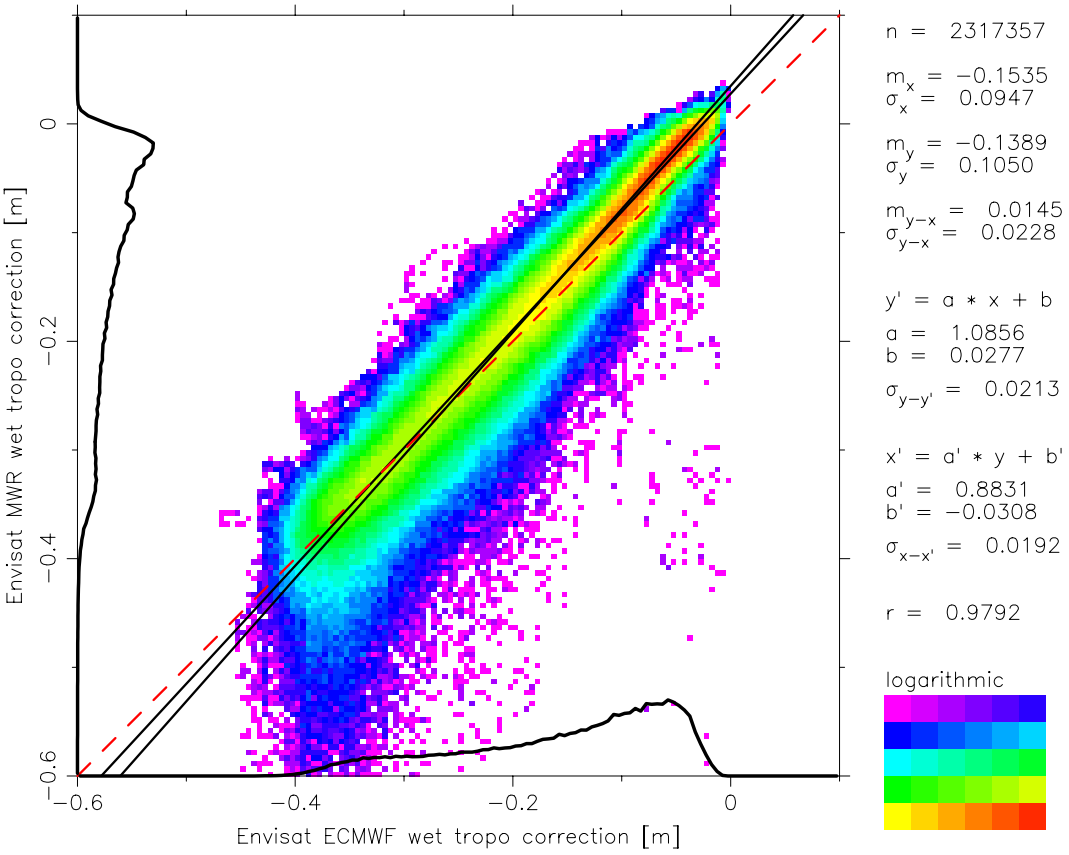

Figure 22. Scattergram of MWR vs. ECMWF wet troposphere correction for Envisat.

In Figure 22 we compare the MWR wet correction from Envisat with the ECMWF model wet for Envisat. Again, it is apparent that the radiometer wet values are wetter in the tropics, but drier elsewhere, with a positive bias of 2.7 cm at the origin ('b' values from the y' regression), which is also seen in Figure 21 comparing the Envisat and ERS-2 MWR wets. A relative scaling of 8.5% (the 'a' values in the y' regression) is observed between the radiometer and model wet corrections on Envisat, compared to the 12.6% scaling difference of the Envisat MWR vs. ERS-2 MWR wet correction, Figure 21.

The root of the problem in Envisat's MWR wet correction is in the algorithm for computing it from the 23.8 and 36.5 GHz brightness temperatures and the Ku-band backscatter. Apparently the algorithm specifies that 1 dB should be removed from the backscatter values in the GDR prior to computing the wet troposphere correction from the following formula:

$$wet_{MWR} = a_0 + a_1 \times \ln(280\text{-}BT_{23.8}) + a_2 \times \ln(280\text{-}BT_{36.5}) + a_3 \times (1/\sigma_0^2) \quad [1]$$

The Envisat GDR processing which generated the CCVT data sets did *not* apply the 1 dB offset to the backscatter values, resulting in the offsets, scale differences, and positive MWR values reported here. Clearly the absolute biases in σ_0 and its impact on the computation of the MWR wet must be consistent with the algorithm shown above and the calibration constants $a_0 - a_3$ that are implemented.

Another, albeit smaller, source of the discrepancy between the Envisat and ERS-2 MWR wet troposphere corrections lies with the two radiometer brightness temperature (BT) values. The scattergrams of the 23.8 GHz and 36.5 GHz BT values for Envisat vs. ERS-2 are presented in Figure 23. Note that the ERS-2 23.8 GHz BTs have been corrected for the known gain loss near the beginning of the mission, and have also had the recommended correction for instrument drift applied. We observe relative biases in the BT values of several degrees Kelvin between the two missions (for example comparing the mean values at the two radiometer frequencies, m_x vs. m_y). The cross-calibration of the Envisat radiometer needs to account for these differences, as well as the backscatter bias/calibration, prior to finalizing the algorithm constants used in Equation 1 above.

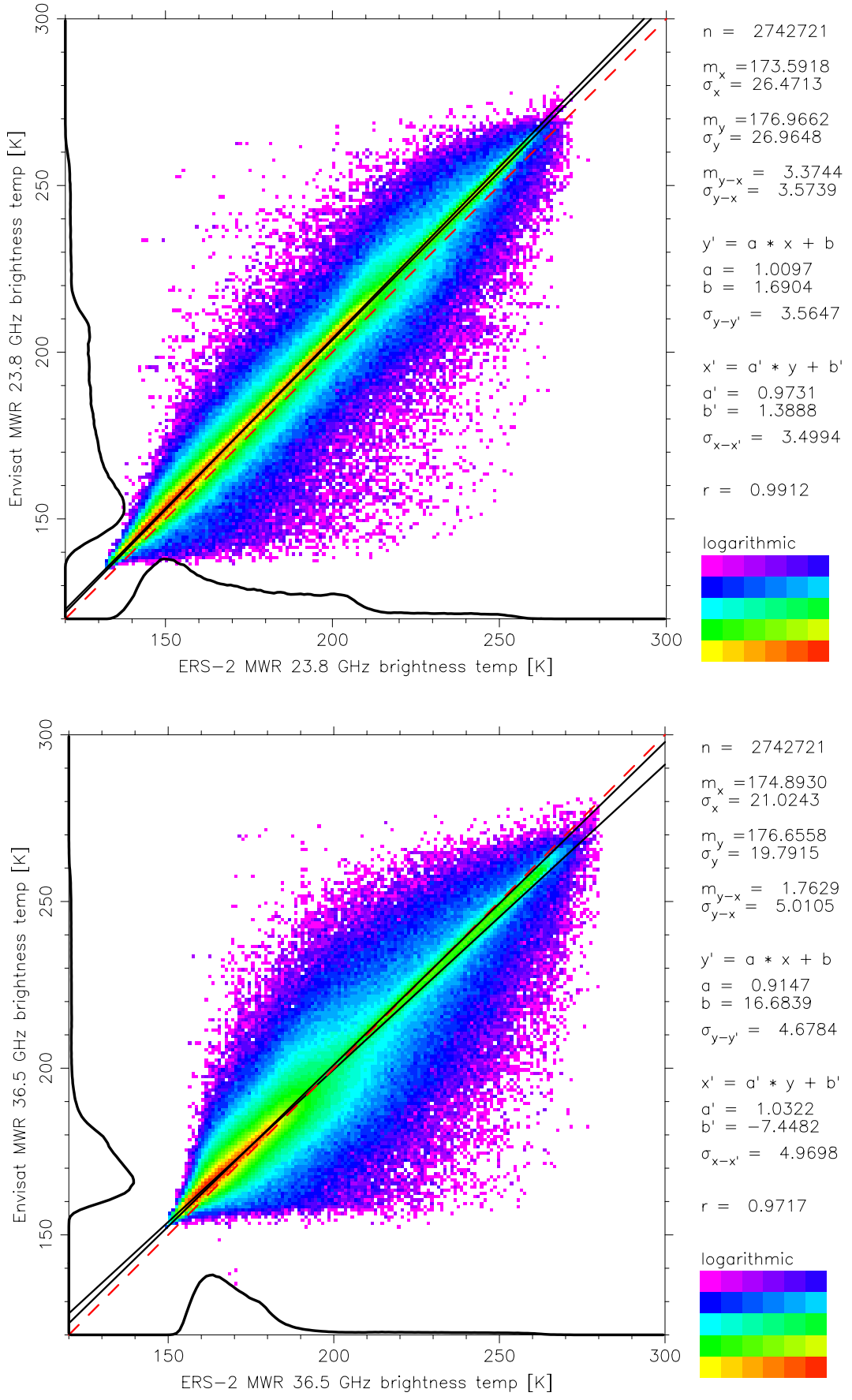

Figure 23. Scattergram of brightness temperatures at 23.8 & 36.5 GHz: Envisat vs. ERS-2.

5.3. Ionosphere Correction for Envisat

Rather than validate the Envisat ionosphere against the ERS-2 data, which is based on the old Bent model, we have chosen in this section to compare three possible ionosphere corrections for Envisat alone. We compare the smoothed dual-frequency correction derived from the altimeter with the DORIS dual-frequency ionosphere model and an independent GPS-based Global Ionosphere Model (GIM) generated by NASA/JPL.

Because of the 12 hour difference in local solar time of the equator crossings (10:00 on descending tracks and 22:00 on ascending tracks) the spatial distribution maps for this correction are broken into separate ascending and descending plots. Presumably, the best ionosphere correction comes from the smoothed altimetric dual-frequency measurement, which is coincident in time with the range measurement. Both the DORIS and GIM corrections are based on 'shell' models of the ionosphere using slant range delays from DORIS tracking and GPS satellites, respectively. However, since the dual-frequency ionosphere is to be calibrated separately (similar to the radiometer wet troposphere discussed above) we do not use this correction in the sea surface height analyses which follow.

The one-dimensional histograms of the three ionosphere corrections (Figure 24) clearly illustrate that the DORIS model has an unrealistically limited dynamic range compared to the other two. The JPL-GIM model underestimates the ionosphere correction relative to the dual-frequency, but has a much more realistic histogram for both ascending and descending passes.

Figure 25 compares the global distribution of the three ionosphere corrections on ascending tracks for Envisat cycle 11, while Figure 26 presents the comparison for descending tracks. We chose cycle 11 due to the better overall coverage, and because if did not suffer the so-called 'S-band anomalies' that plagues cycle 10. The most obvious feature of these two figures is that the DORIS model is clearly not capturing the proper amplitude of the ionosphere correction for either ascending or descending passes. By contrast, the JPL-GIM model does a reasonably good job of emulating the 'true' dual-frequency ionosphere. A useful exercise at this point would be a comparison between the Jason-1 dual-frequency ionosphere values with Envisat, after carefully accounting for differences in altitude and (if possible) minimizing the local solar time differences in the two mission's ground tracks.

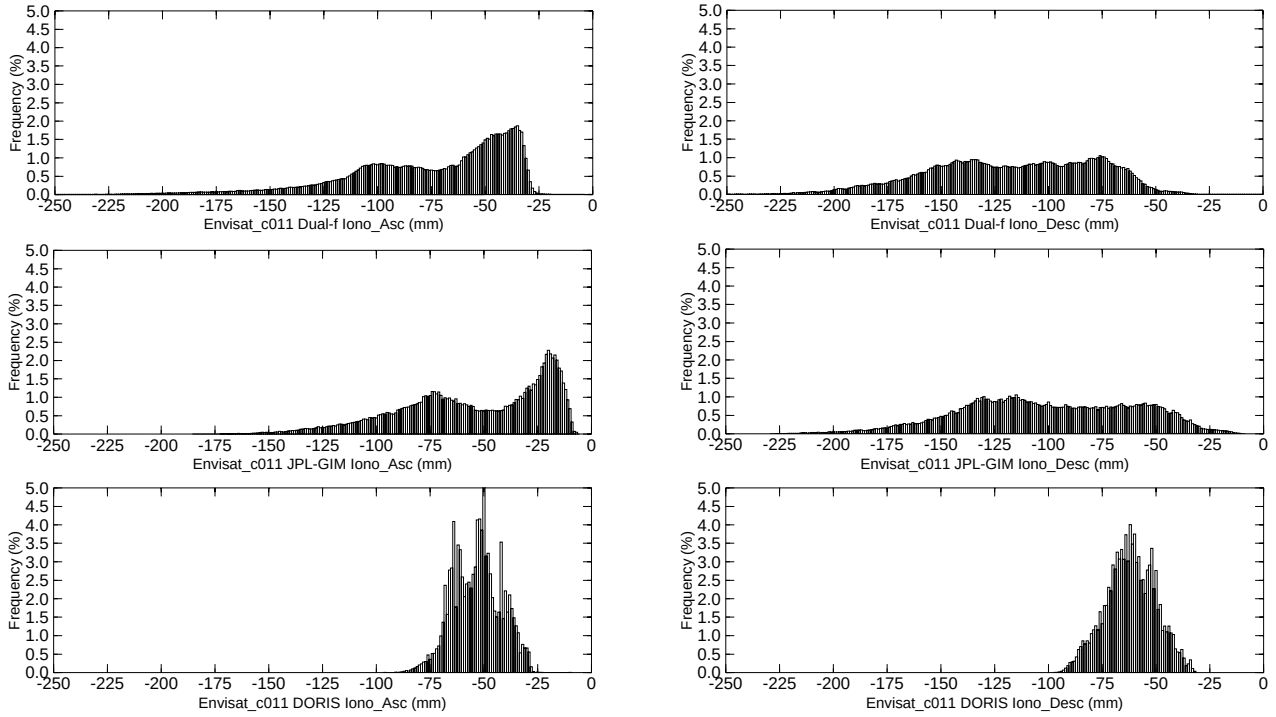

Figure 24. Histograms of ionosphere corrections for Envisat cycle 11. Ascending (L) and Descending (R).

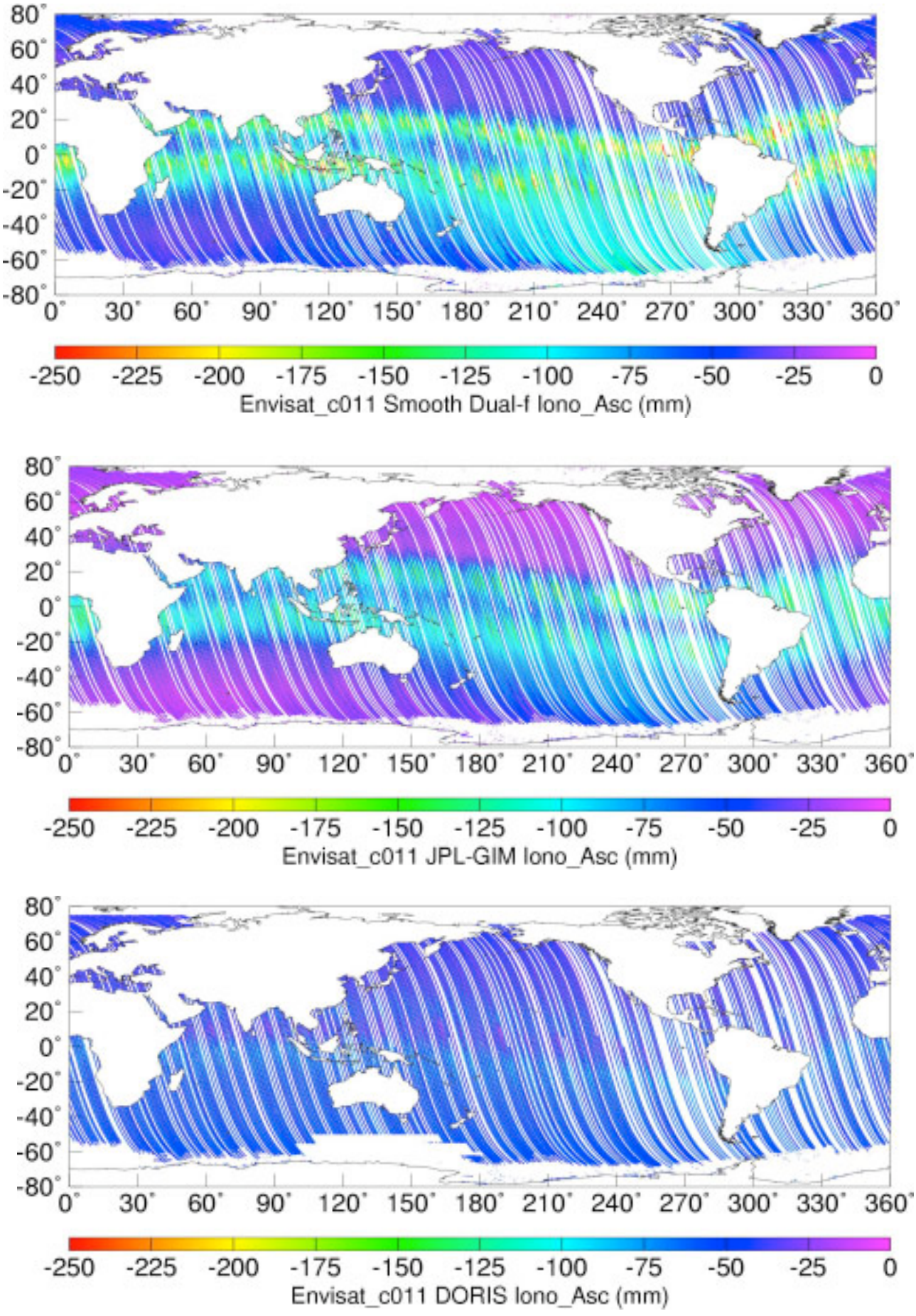

Figure 25. Ionosphere corrections for Envisat ascending passes: cycle 11.

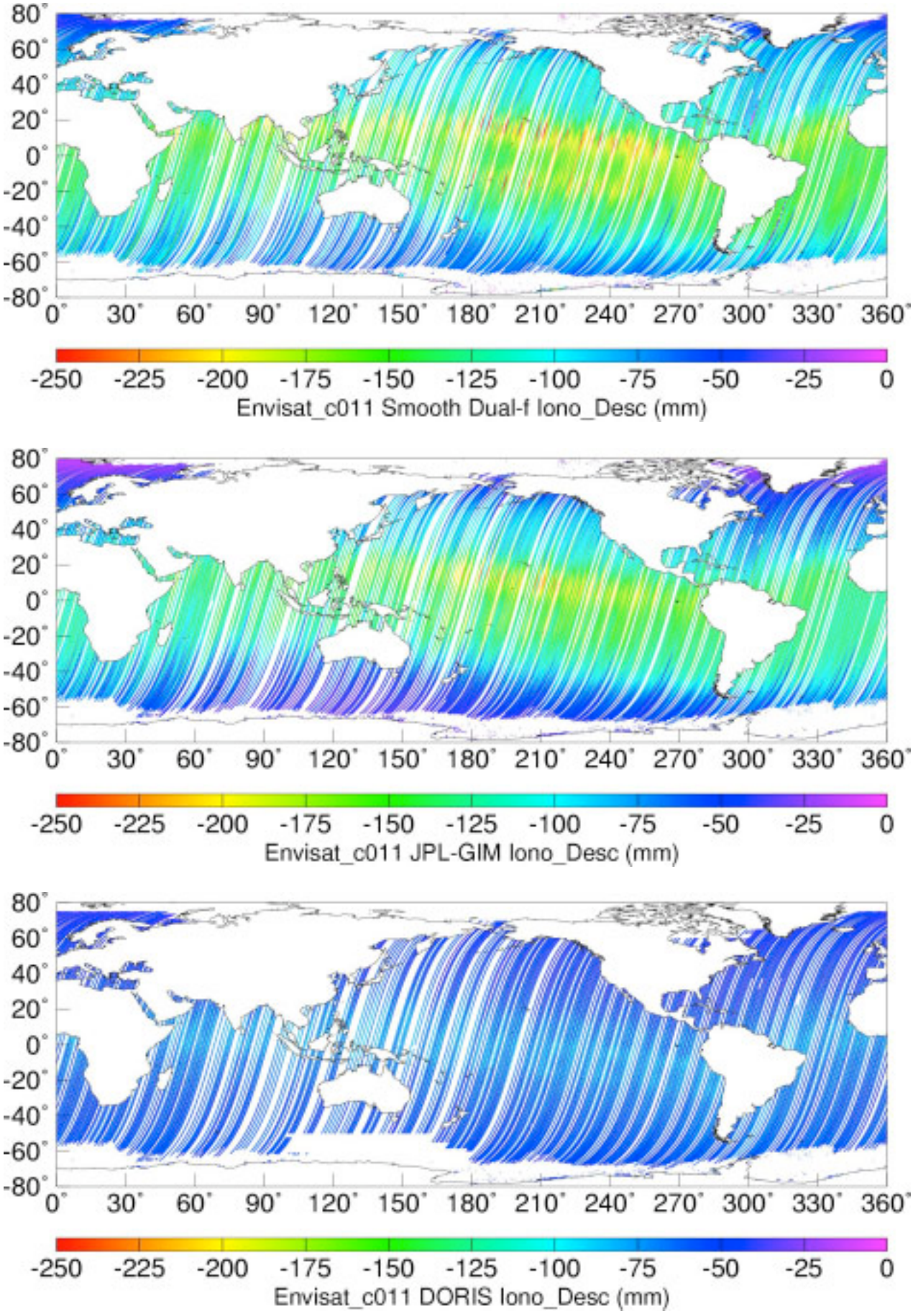

Figure 26. Ionosphere corrections for Envisat descending passes: cycle 11

The scattergrams in Figure 27, over all of cycles 10-12 (both ascending an descending) further illustrate the reduced dynamic range in the DORIS ionosphere compared to the JPL-GIM model, which is common to both panels. The entire distribution of the dual-frequency ionosphere (upper panel) is clearly biased to larger negative values compared to the JPL-GIM model, as observed in the maps in Figures 25 and 26. An external reference from ionosondes is required to determine if the dual-frequency values or the JPL-GIM values are on average closer to the 'truth'.

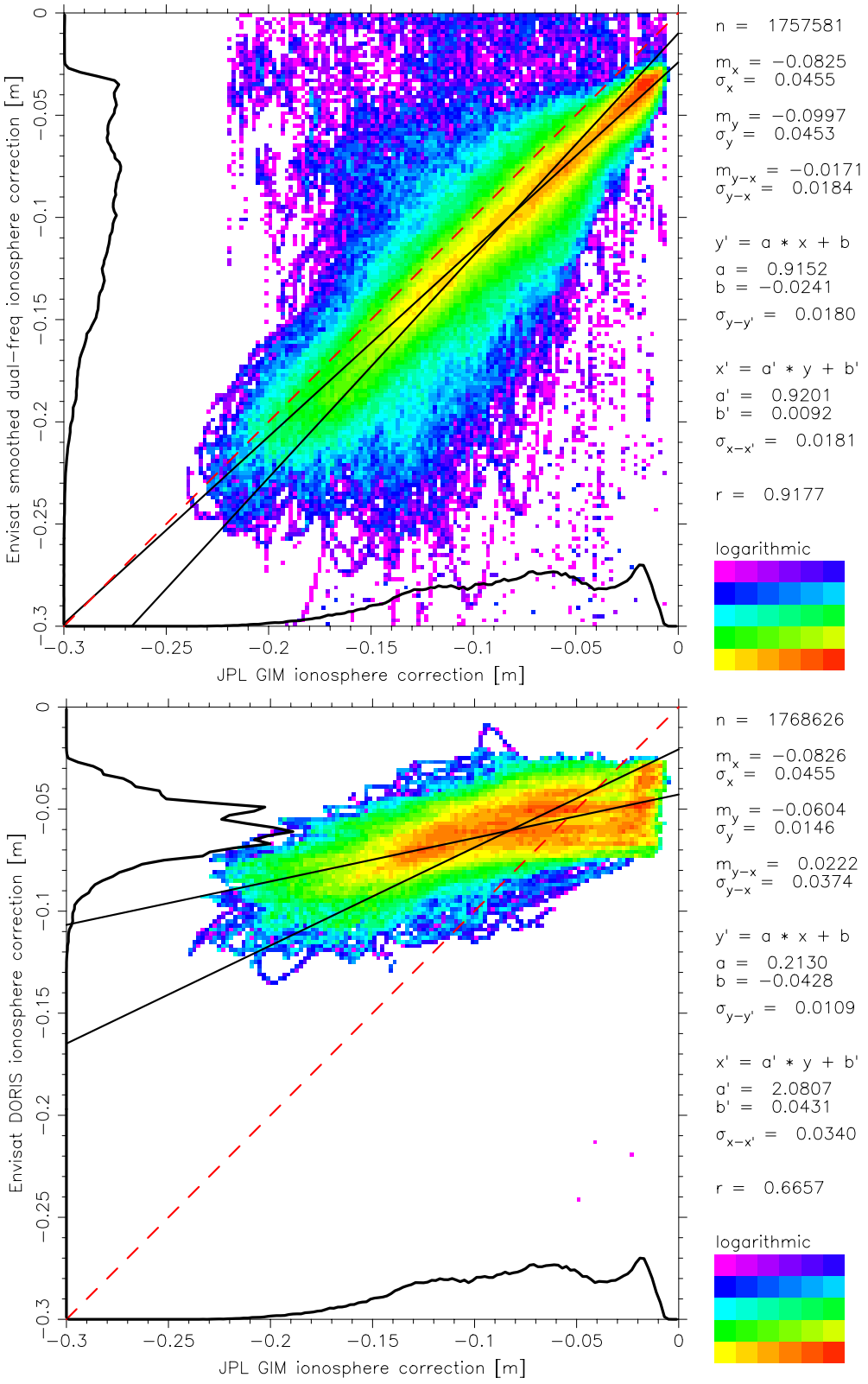

Figure 27. Scattergram of Dual-frequency and DORIS ionosphere corrections vs. JPL-GIM.

6. Sea Surface Height

Finally we reach the end product of the range calibration exercise: sea surface height (SSH) anomalies relative to a mean sea surface (CLS MSS01) and differences in sea surface height between Envisat and ERS-2. After applying edit criteria as discussed in Section 2, and removing from the range the environmental corrections discussed in Section 5, the sea surface height anomaly is simply the difference: orbit height – corrected range – mean sea surface.

We first present in Figure 28 the Envisat SSH anomalies relative to the mean sea surface (MSS). Note that the vertical color scale has been shifted by 1.2 meters to accommodate the majority of the initial uncalibrated height bias in range. Figure 29 similarly portrays the ERS-2 SSH anomalies, which are centered roughly on a 0.1m bias relative to the MSS.

We immediately note that the Envisat and ERS-2 SSH fields agree extremely well in terms of global feature distribution, as well as in the evolution of the height field from one 35-day repeat cycle to the next. This underlines the high quality of the DEOS orbits applied to both datasets, as no obvious 'stripiness' is evident in either mission's height fields. From this pair of Figures we can roughly estimate the relative bias between Envisat and ERS-2 at 1.1 meter. As discussed at the final CCVT meeting, 73.68 cm of this bias is a 'known problem' in one of the characterization tables used to generate the Envisat GDRs. Hence, the true relative bias is on the order of 37 cm. In Figure 30 the SSH differences between Envisat cycles 10 - 12 relative to ERS-2 cycles 78 - 80, respectively, are presented in map form. Generally the differences exhibit the long-wavelength orbit errors present in both datasets, but there is some indication of a geographically correlated systematic error between Envisat and ERS-2. This may be due to systematic orbit differences (*e.g.,* through the introduction of DORIS tracking data) or related to differences in the sea state bias, which we will deal with in Section 7. The vertical color bar in this figure is centered near the mean relative bias at 1.125 m.

In the following discussion, the 73.68 cm bias is accounted for by adding it to the Envisat ranges.

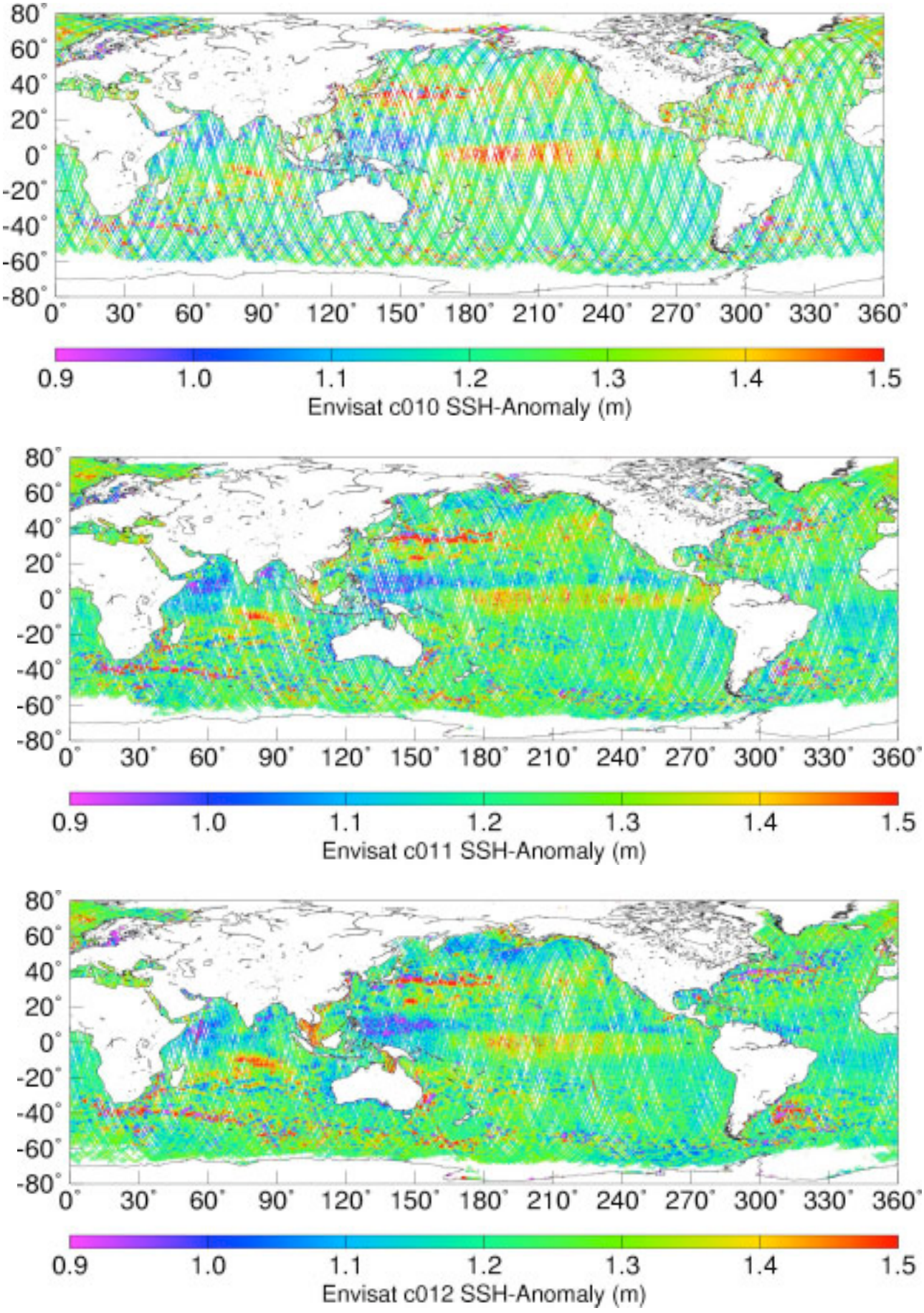

Figure 28. Sea surface height anomalies relative to CLS mean sea surface for Envisat cycles 10-12.

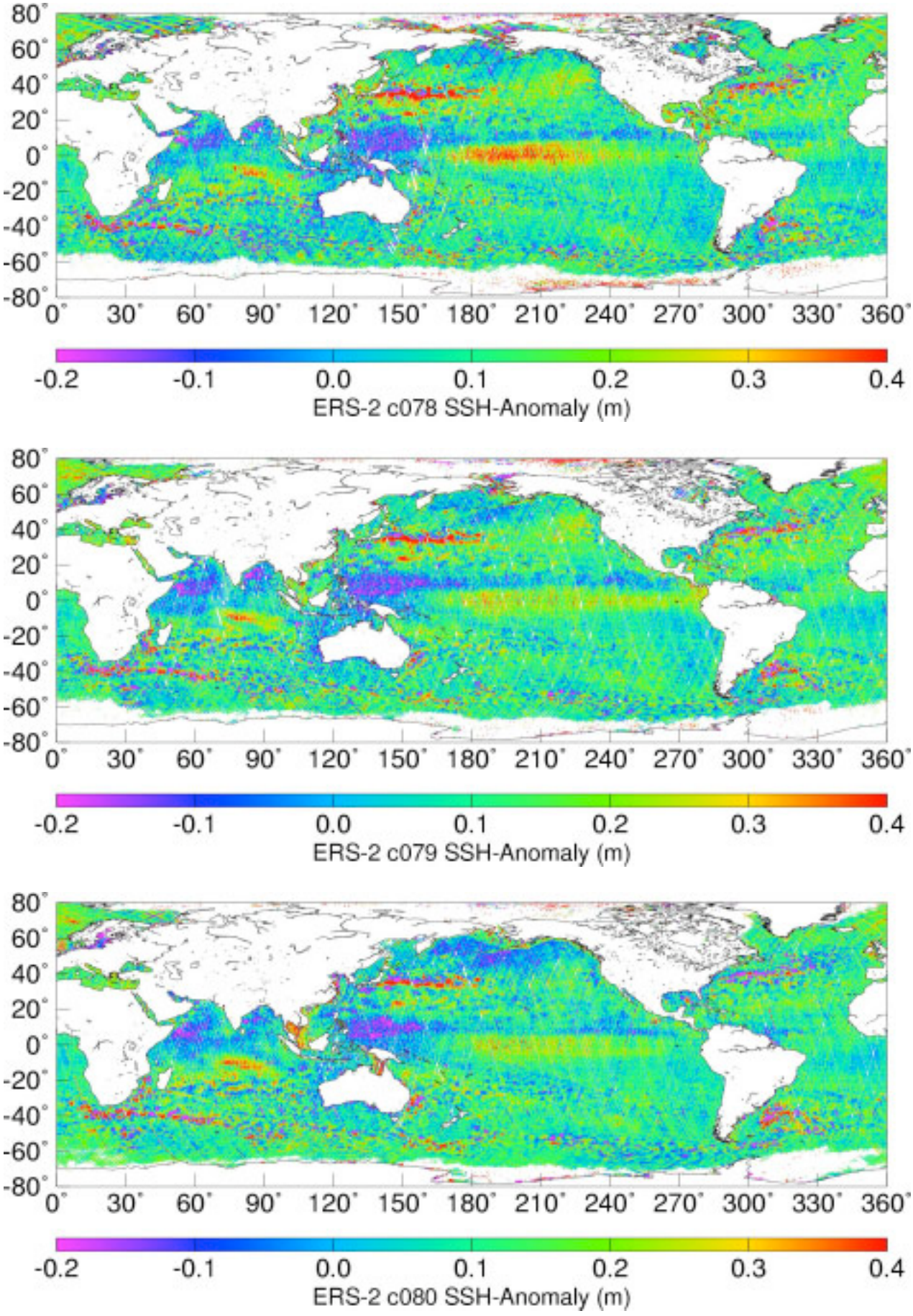

Figure 29. Sea surface height anomalies relative to CLS mean sea surface for ERS-2 cycles 78 – 80.

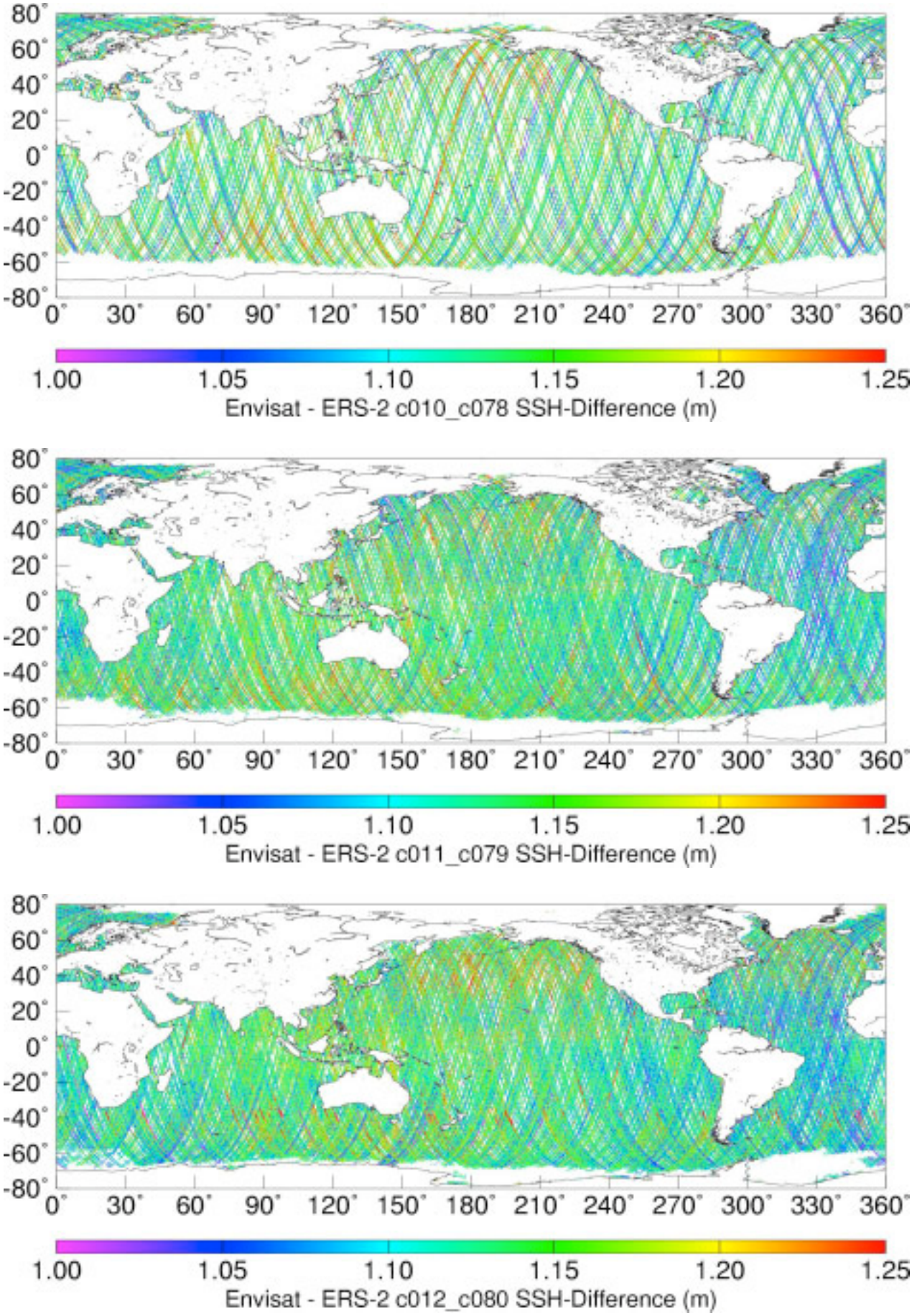

Figure 30. Sea surface height differences: Envisat - ERS-2.

7. Creation of Sea State Bias Models

The Sea State Bias (SSB) correction is one of the most uncertain factors in the calibration of the Envisat altimeter range. There is no reason to assume that the altimeter range measured by ERS-2 and Envisat are equally affected by waves and wind. Besides, we have shown that ERS-2 and Envisat measure particularly different wave heights. For both reasons we have to create a new SSB correction model for Envisat.

For the cross-calibration using collinear tracks of ERS-2 and Envisat, we can take advantage of the short time delay between the measurements by the two satellites. In this short time interval the sea surface height and most of the altimeter range corrections should be roughly the same. The sea surface height difference (after applying the corrections mentioned in Table 1, except for the SSB correction) reflects the difference between the SSB correction of ERS-2 and Envisat. Note that the Envisat values of wet troposphere delay were multiplied by 0.958 to reflect the difference with the ERS-2 values (see Section 5.1).

The sea surface height differences are forthwith mapped onto a rectangular grid with the Envisat wind speed and significant wave height as coordinates. The grid spacing is 0.25 m/s and 0.25 m, respectively. The average sea surface height difference (Envisat – ERS-2) in each grid cell becomes a measure of sea state bias difference between the two altimeters at the particular wave height and wind speed. Since the outer reaches of the grid are not densely populated, and to reduce the noise within the grid, the grid is manipulated after the averaging.

First, a bias and BM4 model is fitted to the grid values, taking into account the number of points and the variance in each grid point. This results in the solution of 5 parameters (a_0 through a_4).

$$a_0 + \mathrm{SWH}\,[a_1 + a_2\,U + a_3\,U^2 + a_4\,\mathrm{SWH}] \qquad [2]$$

The residuals after the fit are first smoothed and added to the BM4 model, while a_0 is set to zero since the SSB correction should be (on average) zero at zero wave height. Figure 31 shows the hybrid ΔSSB model that was determined from the ERS-2 and Envisat data over the 3 cycles. Note that in the data dense region, the SSB differs by ±2 cm, a significant amount if ignored.

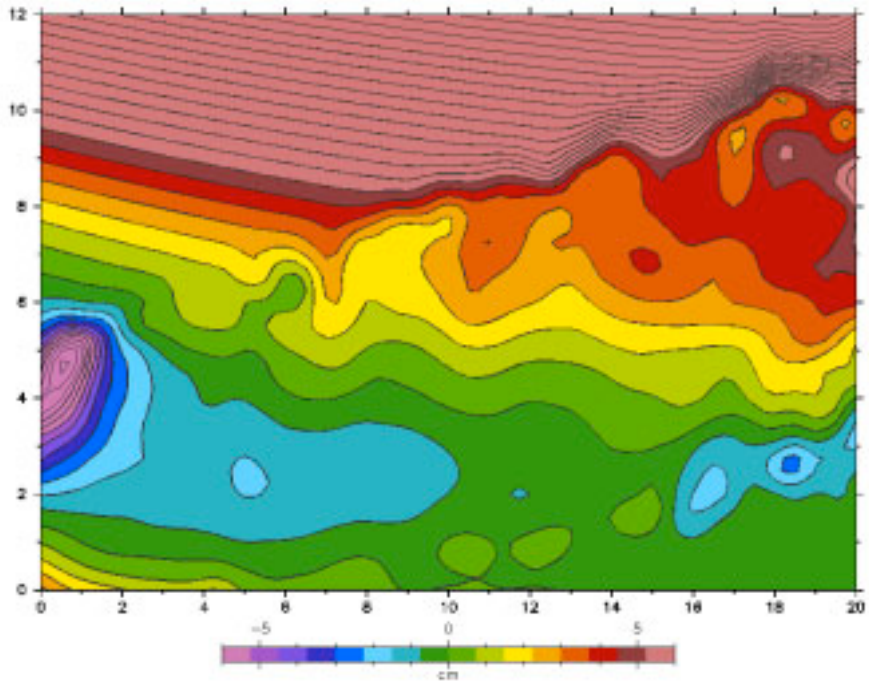

Figure 31. Hybrid ΔSSB (Envisat – ERS-2) model. Horizontal scale is wind speed in m/s; vertical scale is significant wave height in m.

It must be noted that this model is *neither* a correction for the SSB of Envisat, *nor* for ERS-2. It should also *not* be seen as the difference between the SSB of Envisat and ERS-2. The model reflects, instead, the difference in sea state bias after the wave height and wind speed of ERS-2 are assumed to be those measured by Envisat. It is sensible to use Envisat as the 'gold standard' since we know that the wave heights of ERS-2 are not as accurate as those of Envisat.

In a similar way, the hybrid SSB models for both ERS-2 and Envisat were computed. In this case the sea height residuals over the MSS CLS01 were used as input. The two models are shown in Figure 32

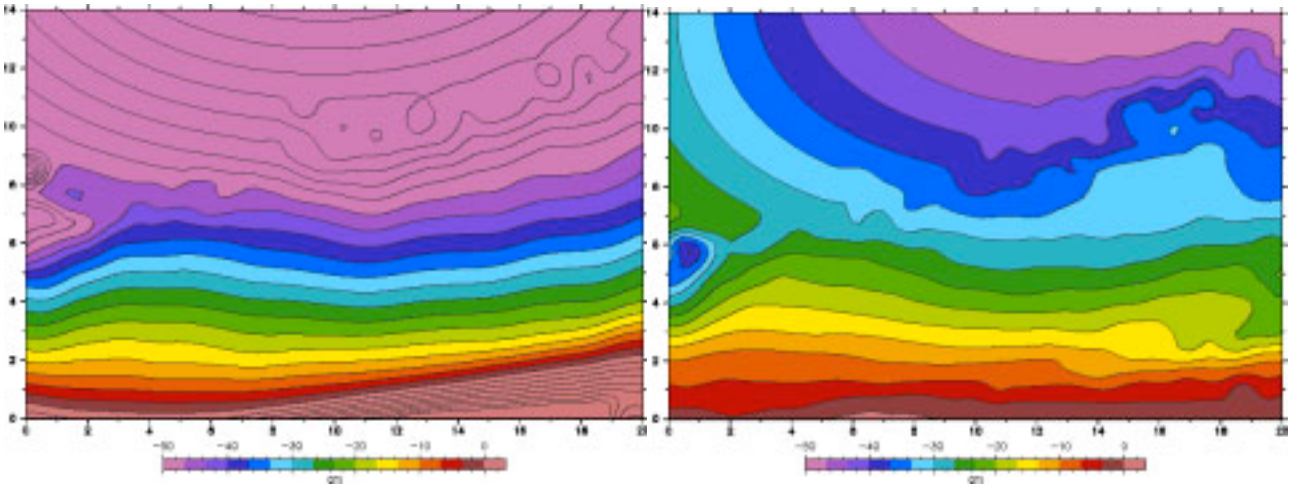

Figure 32. Hybrid SSB models for ERS-2 (left) and Envisat (right). Horizontal scale is wind speed in m/s; vertical scale is significant wave height in m.

8. Spectral analyses

Maybe as important as the biases in the range, significant wave height and backscatter are their spectral behavior in comparison with other altimeters. It is important to verify whether the Envisat altimeter captures details in the sea surface height, significant wave height and backscatter at the same, or better, horizontal resolution as other altimeters.

To analyze the performance of the Envisat (and other) altimeters at short wave lengths, we have simply computed one-dimensional spectra of sea surface height residuals (compared to MSS CLS01), significant wave height and backscatter. The results for Envisat, ERS-2, TOPEX, and Jason-1 are compared in Figure 33.

Envisat shows the lowest range noise level of all altimeters (around 4 cm, note that this includes noise in the MSS CLS01 model). The lower value of TOPEX should be ignored since it is clearly smoothed below wavelengths of about 8 seconds (50 km).

Envisat shows a similarly good performance in terms of significant wave height. The noise level is about 22 cm. The smoothing of TOPEX measurements at shorter wavelengths is again evident.

The registration of backscatter is very similar among ERS-2, Jason-1 and Envisat. Again, TOPEX is the odd one out, showing much more power (hence noise) over the entire range of wavelengths.

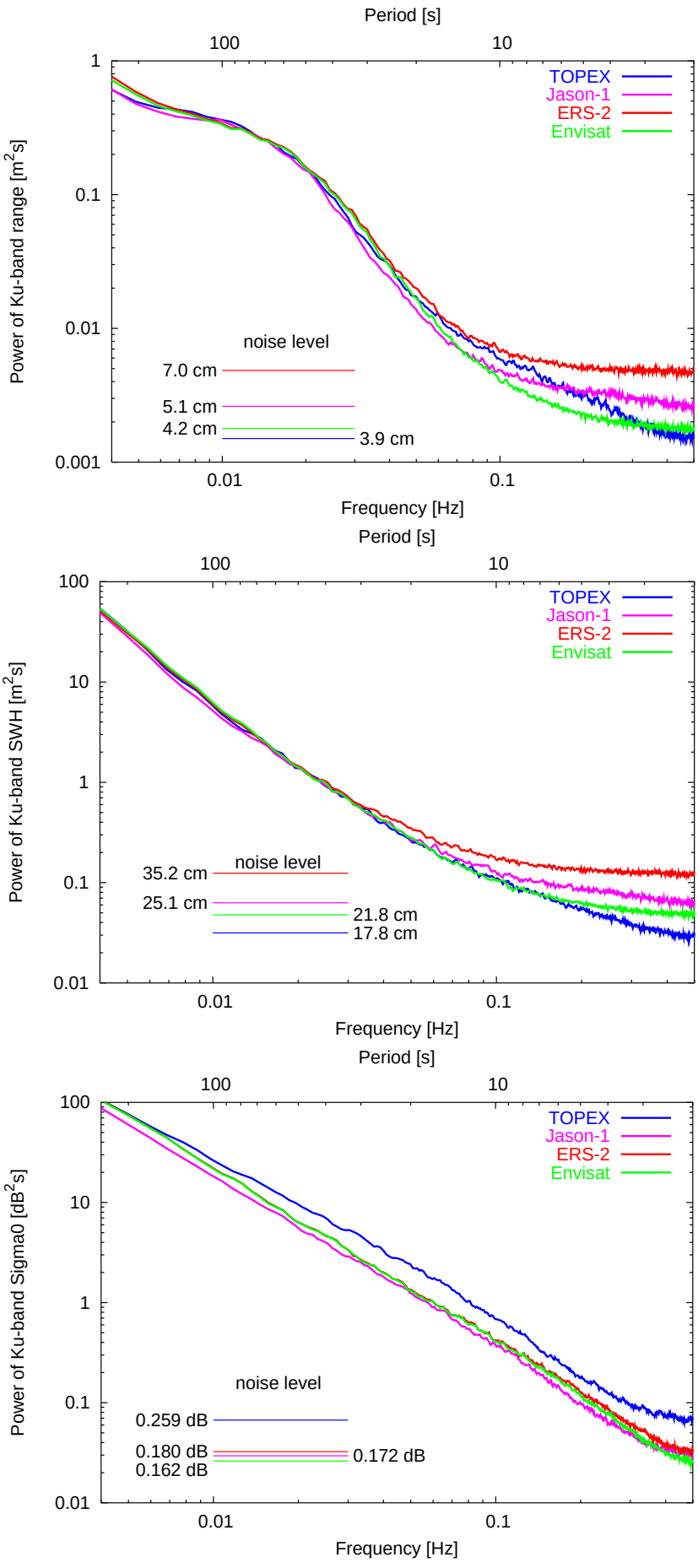

Figure 33. One-dimensional spectra of sea surface height residual (top), significant wave height (middle) and backscatter coefficient (bottom).

9. Cross-calibration results

The top half of Table 4 lists the statistics of the sea surface height residuals of Envisat and ERS-2 for each of the cycles that were investigated, as well as the overall statistics for the three cycles. The poorer statistics for Envisat cycle 12 are mainly due to orbit errors around the time that the DORIS instrument was switched off. From these numbers we can conclude that (a) the relative sea surface heights are precise to within about 11 cm for both altimeters and (b) the relative range bias is approximately 38.7 cm. It should be noted, however, that the SSB for Envisat is not yet tuned in this analysis.

The second half of Table 4 shows the statistics of the sea surface height differences between Envisat and ERS-2 along collinear tracks. Evidently, the standard deviation is much smaller, giving a more accurate estimate of the relative range bias. The two cases listed assumed that either the SSB of the two altimeters is the same (case 3) or that the difference between the respective SSBs is well represented by the model developed in Section 7 (case 4). Note that there is an approximate 7 mm difference between the two bias estimates, demonstrating that the development of a good SSB model for Envisat is important. The histograms of cases 3 and 4 are shown in Figure 34. The grey histogram refers to case 3, the red histogram to case 4.

In order to evaluate whether the time tags of Envisat may be biased compared to ERS-2, we have created a scattergram of the ΔSSH against the orbital altitude rate, Figure 35. In such a diagram the best fitting line indicates both the relative range bias (its intercept) and the relative timing bias (its tilt). The relative range bias (37.23 cm) is the same as found in Table 4 (case 3); the relative timing bias (-0.1 ms) is insignificant.

Table 4. Statistics of sea surface height residuals and collinear track height differences.

Case		Mean ΔSSH (cm)	Std. Dev. ΔSSH (cm)
1) ERS-2 SSH vs. MSS CLS01 Default corrections	Cycle 78	10.1	14.0
	Cycle 79	10.1	11.9
	Cycle 80	9.8	12.4
	All cycles	**10.0**	**12.8**
2) Envisat SSH vs. MSS CLS01 Default corrections	Cycle 10	49.0	12.4
	Cycle 11	48.8	11.8
	Cycle 12	48.2	23.6
	All cycles	**48.7**	**17.2**
3) Envisat – ERS-2 Default corrections, no SSB applied	Cycle 10/78	37.49	6.76
	Cycle 11/79	37.26	6.73
	Cycle 12/80	36.97	6.56
	All cycles	**37.23**	**6.68**
4) Envisat – ERS-2 Default corrections, ΔSSB applied	Cycle 10/78	38.18	6.69
	Cycle 11/79	37.91	6.65
	Cycle 12/80	37.68	6.49
	All cycles	**37.92**	**6.61**

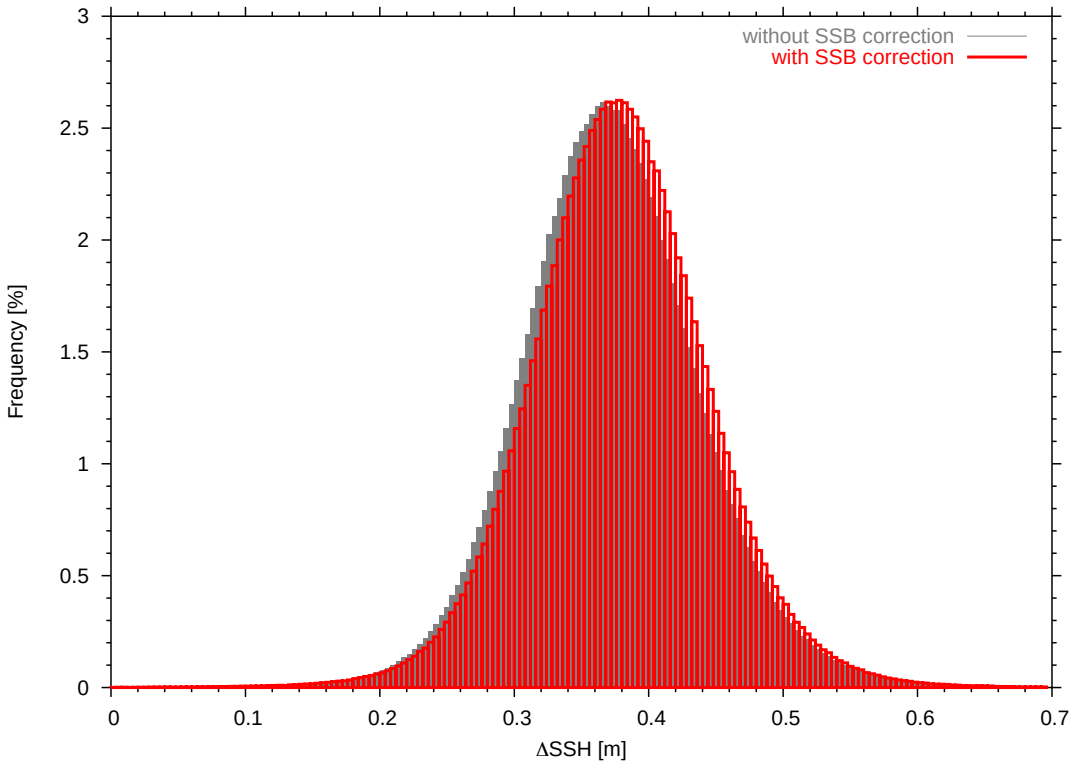

Figure 34. Histogram of the sea surface height difference between Envisat and ERS-2 along collinear tracks. Two cases are shown: without using SSB correction (in grey) or using the ΔSSB model (in red).

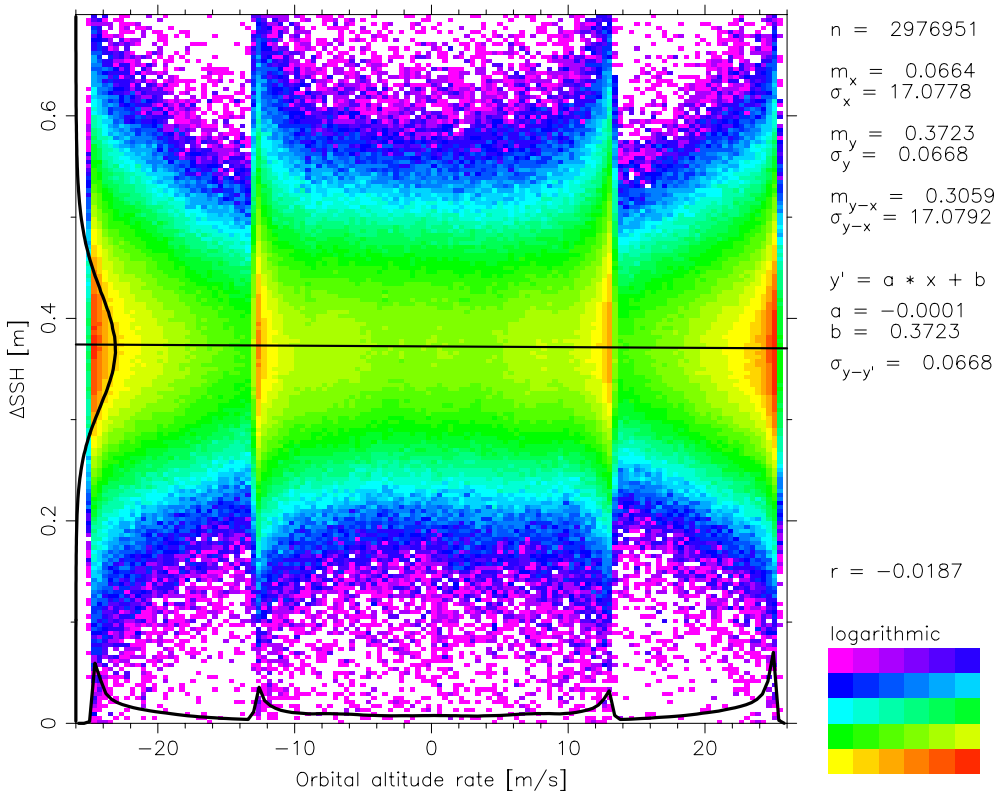

Figure 35. Scattergram of ΔSSH (Envisat – ERS-2) against orbital altitude rate. A tilt in the best fit indicates a timing bias difference.

In order to compare Envisat sea surface heights with other satellites, we need to use dual-satellite crossovers. The mean height difference is then representative of the relative altimeter range bias. Table 5 lists the mean and standard deviation of Envisat crossovers as well as a number of dual-satellite combinations. The sensitivity to different orbit solutions is tested.

From this Table we can draw the following conclusions:

1. The Envisat single satellite crossovers (maximum time interval 17.5 days) has a standard deviation of about 9 cm, which is similar to TOPEX and ERS-2 for a similar time interval.
2. Judging from the standard deviation of the Envisat single satellite crossovers, the DEOS GRIM5-C1 orbits perform significantly better than the CNES orbits provided on the Envisat GDRs. This result is confirmed by the Envisat/Jason-1 crossover analysis.
3. The relative bias between Envisat and ERS-2 is about 38.5 cm (when their respective, but not consistent SSB models are used).
4. Given the rise of the standard deviation of the Envisat – ERS-2 crossovers when not using both GRIM5-C1 orbits, it appears essential that both orbit solutions should be consistent.
5. The relative range bias of Envisat with respect to GFO, Jason-1 and TOPEX is approximately 44.5 cm, 37.5 cm and 48.0 cm, respectively.

Table 5. Statistics of single and dual-satellite crossovers.

Altimeter 1	Altimeter 2	Mean crossover difference (cm)	Std. dev. crossover difference (cm)
Envisat (asc) Default corrections	**Envisat (des)** Default corrections	0.31	8.99
Envisat (asc) CNES orbits	**Envisat (des)** CNES orbits	-0.52	9.46
Envisat Default corrections	**ERS-2** Default corrections	38.53	9.46
Envisat Default corrections	**ERS-2** DGM-E04 orbit	39.03	9.91
Envisat CNES orbit	**ERS-2** Default corrections	38.57	9.70
Envisat Default corrections	**GFO** Default corrections	44.52	9.35
Envisat Default corrections	**Jason-1** Default corrections	37.48	7.40
Envisat CNES orbits	**Jason-1** Default corrections	37.38	7.73
Envisat Default corrections	**TOPEX** Default corrections	47.99	7.12

10. Conclusions and Recommendations

10.1. Main conclusions

Three cycles of Envisat GDR data were validated and calibrated against near-coincident precise altimeter data of ERS-2, GFO, TOPEX and Jason-1.

During the validation process a number of minor errors in the Envisat GDR data were discovered, plus a number of issues that require enhancement or reconsideration in the next (official) release of the data. At the same time edit criteria for the selection of accurate, uncontaminated sea surface height measurements were constructed.

Based on three cycles of Envisat GDR data, we were able to compute relative range biases compared to other satellite altimeters within an error margin of a few centimeters. An important factor in the cross-calibration of the altimeter range is the correction for the sea state bias. A hybrid model that captures the difference between the Envisat and ERS-2 sea state bias was developed.

Taking into account this improved model of the sea state bias, Envisat measures ranges about 38.0 cm short of ERS-2.

The significant wave height measurements of Envisat have a higher quality than those of ERS-2. ERS-2 underestimates wave heights by about 22 cm; at low wave heights the values get clipped to 0 cm. The backscatter coefficients of ERS-2 and Envisat are nearly identical and have an insignificant bias.

The spectral analyses showed that Envisat provides higher resolution along-track sampling of sea surface height and wave height than any of the currently flying satellite altimeter. The performance in backscatter is comparable to other current altimeters.

10.2. Recommendations

A number of recommendations were generated at the CCVT meeting and within this report. It is essential that these recommendations should be considered as soon as possible. The GDR data quality and usability would significantly benefit from the incorporation of these upgrades:

1. *Editing & Flags*
   a. Do not set the MWR_Land flag when no MWR data are available. Such practice would cause users to throw away data even when using the model wet troposphere correction.
   b. Do not set the Alt_Rain flag when no MWR data are available. Such practice makes users throw away all data when the MWR is not on, even when the model wet troposphere is available as an alternative correction.
   c. Try to formulate a rain probability index vs. the currently used binary rain flag.
   d. Compute the rain flag (or probability) even when there is no MWR data; set a new flag to indicate when the rain flagging is based on backscatter attenuation alone or both backscatter and MWR.
   e. Add peakiness to the MAR products to aid with sea-ice editing.
   f. Use backscatter attenuation information to flag ‘S-band anomalies’.

2. *SWH, Wind, Sigma-0*
   a. Replace unsigned INT with signed INT to avoid zero-clipping of sea surface height measurements
   b. Replace the maximum wind value (20 m/s) with the default value.

c. Carefully account for the 3.5 dB (already applied), 1 dB (absolute calibration recommendation) and 1 dB correction to sigma-0 that goes into the MWR wet correction and wind speed *before* finalizing the algorithm coefficients.
d. Investigate the source of the '1 m/s' class in the wind speed histogram. Develop a new wind model *after* all sigma-0 calibrations have been corrected and accounted for.

3. *Dry troposphere and inverse barometer*
   a. Let users be aware that Envisat GDRs have the inverse barometer correction based on the local minus global mean pressure, whereas ERS-2 OPR users are likely to base the inverse barometer correction on local pressure minus 1013.3 mbar.

4. *Model and MWR wet troposphere*
   a. **Investigate the source of the ECMWF model wet differences between the ERS-2 OPRs and Envisat GDRs.** Is it a result of spectral/Gaussian versus physical/Cartesian grids? Is it the data source: ECMWF versus FMO? In any case a 4.2% difference in scale should *not* occur.
   b. Check the 'delta-doc' for the IPF (FDGDR) chain vs. the CMA (I/GDR) processing, specifically for these model wet differences.
   c. Cross-calibrate both brightness temperatures *before* evaluating the MWR wet algorithm coefficients (similar to the sigma-0 calibration going into the MWR algorithm).
   d. Monitor the 36.5 GHz brightness temperature drift, since early indications are that the drift is excessive.

5. *Ionosphere*
   a. **The DORIS ionosphere correction needs major tuning/calibration** to be a useful backup to the dual-frequency measurement.

6. *SSB*
   a. A new SSB model needs to be developed. This is preferably a hybrid model, taking into account the following:
      i. Use sigma-0 (perhaps on a linear, vs. log/dB scale) versus wind speed as ordinate.
      ii. Use JPL-GIM (and not the dual-frequency measurement) when computing the direct estimate SSB to avoid cross-contamination.
   b. Initially utilize a direct-estimate SSB until sufficient data exist for a non-parametric model.

7. *General Processing Issues*
   a. Replace the state vector orbit with the DORIS-DIODE orbit in FDMAR and FDGDRs.
   b. Use CLSMSS01 as the mean sea surface model and ensure consistent treatment of the global mean ocean pressure in the inverse barometer correction.
   c. Fix the MCD retracker status flag bits in the CMA chain (OK in the IPF for FDGDRs).
   d. Fix the long-period tide bug in the GDRs.
   e. Strive to eliminate duplicate records in the FD products.
   f. Fix the 'F-PAC anomaly': NaNs in the GDRs.
   g. Fix the sigma-0 atmospheric attenuation correction (currently set to a climatological value).